Theses and Dissertations

Thesis Collection

1986-09

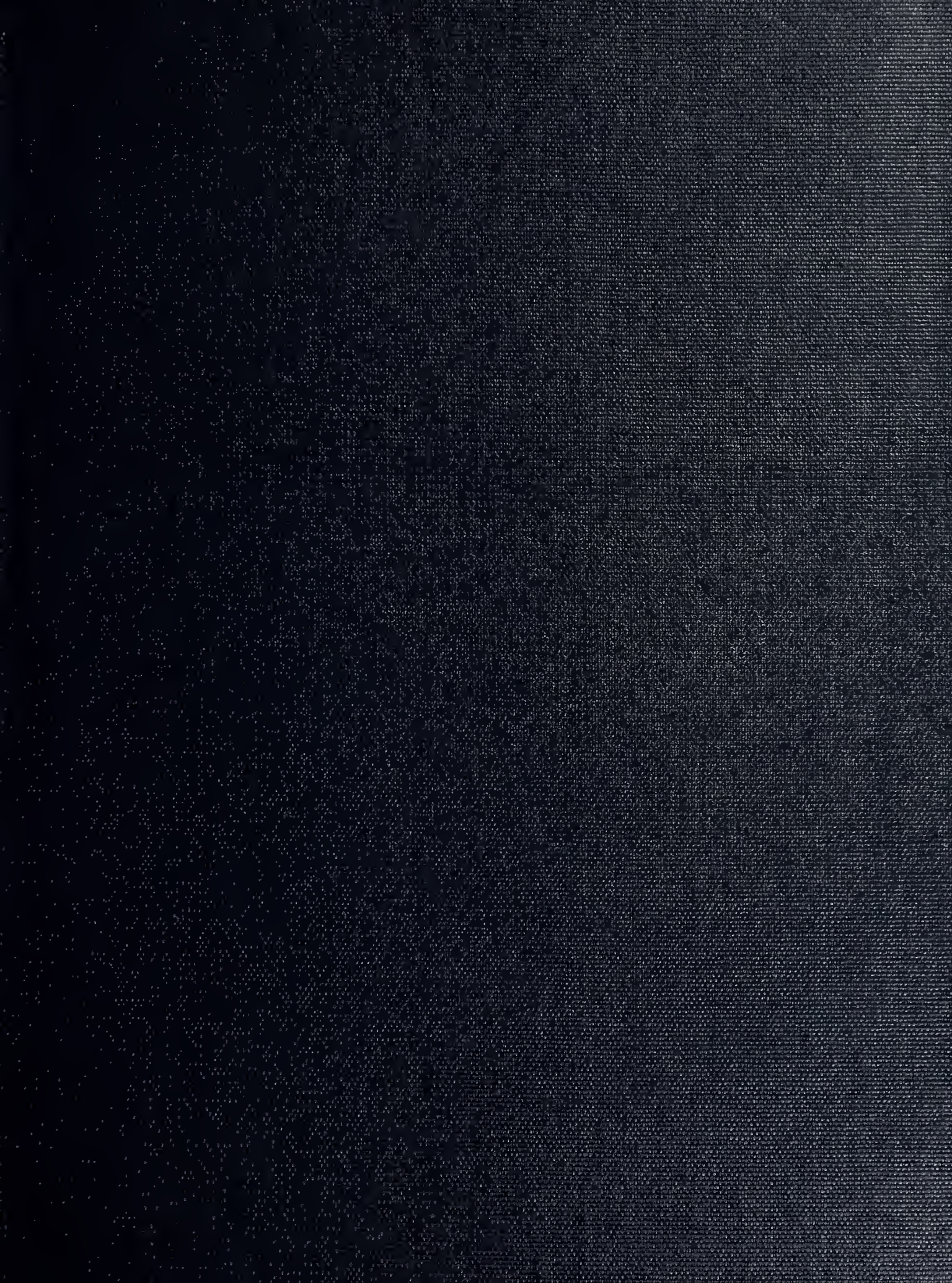# Coastal erosion along the Monterey Bay

McGee, Timothy

http://hdl.handle.net/10945/21711

NAVAL POSTGRADUATE SCHOOL
Monterey, California

THESIS

COASTAL EROSION ALONG MONTEREY BAY

by

Timothy McGee

September 1986

Thesis Advisor:	Edward B. Thornton
Co-Advisor:	Stevens P. Tucker

Approved for public release; distribution is unlimited.

REPORT DOCUMENTATION PAGE

1a. REPORT SECURITY CLASSIFICATION UNCLASSIFIED	1b RESTRICTIVE MARKINGS

2a. SECURITY CLASSIFICATION AUTHORITY	3 DISTRIBUTION / AVAILABILITY OF REPORT
2b DECLASSIFICATION / DOWNGRADING SCHEDULE	Approved for public release; distribution is unlimited.

4. PERFORMING ORGANIZATION REPORT NUMBER(S)	5 MONITORING ORGANIZATION REPORT NUMBER(S)

6a NAME OF PERFORMING ORGANIZATION Naval Postgraduate School	6b. OFFICE SYMBOL (If applicable) 35	7a. NAME OF MONITORING ORGANIZATION Naval Postgraduate School

6c. ADDRESS (City, State, and ZIP Code) Monterey, CA 93943-5000	7b. ADDRESS (City, State, and ZIP Code) Monterey, CA 93943-5000

8a. NAME OF FUNDING / SPONSORING ORGANIZATION	8b. OFFICE SYMBOL (If applicable)	9. PROCUREMENT INSTRUMENT IDENTIFICATION NUMBER

8c. ADDRESS (City, State, and ZIP Code)	10. SOURCE OF FUNDING NUMBERS

PROGRAM ELEMENT NO.	PROJECT NO.	TASK NO	WORK UNIT ACCESSION NO.

11. TITLE (Include Security Classification)

COASTAL EROSION ALONG THE MONTEREY BAY

12. PERSONAL AUTHOR(S)
McGEE, Timothy

13a. TYPE OF REPORT Master's thesis	13b TIME COVERED FROM _____ TO _____	14. DATE OF REPORT (Year, Month, Day) 1986 September	15 PAGE COUNT 90

16. SUPPLEMENTARY NOTATION

17. COSATI CODES			18 SUBJECT TERMS (Continue on reverse if necessary and identify by block number)
FIELD	GROUP	SUB-GROUP	Erosion, waves, photogrammetry, refraction

19. ABSTRACT (Continue on reverse if necessary and identify by block number) Coastal erosion, as inferred by measuring bluff recession is correlated with wave height at 12 sites along the Monterey Bay coastline. Bluff recession rates are established by applying precise photogrammetric techniques to a 44-year time series of aerial photographs. Wave heights are determined from the U.S. Army Corps of Engineers Wave Information Studies spectral wave climatology, where deep water gravity waves are hindcast from historic wind fields at three-hour intervals from Jan 56-Dec 75. The deep water spectra are refracted to shallow water spectra at a nominal depth of 4m. An erosion model is developed for Monterey Bay where the erosion process is modelled as a non-linear function of the 4-m significant wave height:

$$R = [AHs^2 + BHs + C(Tide + 1.02Hs - Clifftoe)]/Beach\ Slope$$

The coefficients A,B,C are computed from a least squares regression of the modelled and observed recession rate values. The erosion model provides a reasonable representation of the erosion process in Monterey Bay, where the mean standard error between observed and modelled erosion rates is $\pm$ 0.17 m/yr. Adjustment of the wave energy coefficient, A, allows tuning of the model for high and low wave energy locations.

20. DISTRIBUTION / AVAILABILITY OF ABSTRACT ☒ UNCLASSIFIED/UNLIMITED ☐ SAME AS RPT ☐ DTIC USERS	21. ABSTRACT SECURITY CLASSIFICATION UNCLASSIFIED

22a NAME OF RESPONSIBLE INDIVIDUAL E.B. THORNTON	22b TELEPHONE (Include Area Code) 408-646-2847/2552/2673	22c. OFFICE SYMBOL 68Tm

DD FORM 1473, 84 MAR   83 APR edition may be used until exhausted.   SECURITY CLASSIFICATION OF THIS PAGE
All other editions are obsolete

Coastal Erosion along Monterey Bay

by

Timothy McGee
Lieutenant, United States Navy
B.S., U.S. Naval Academy, 1978

Submitted in partial fulfillment of the
requirements for the degree of

MASTER OF SCIENCE METEOROLOGY AND OCEANOGRAPHY

from the

NAVAL POSTGRADUATE SCHOOL
September 1986

ABSTRACT

Coastal erosion, as inferred by measuring bluff recession is correlated with local wave height at twelve sites along the Monterey Bay coastline. Bluff recession rates are established by applying precise photogrammetric techniques to a 44-year time series of aerial photographs. Wave heights are determined from the U.S. Army Corps of Engineers Wave Information Studies spectral wave climatology, where deep water gravity waves are hindcast from historic wind fields at three-hour intervals from January 1956 to December 1975. The deep water spectra are refracted to shallow water spectra at a nominal depth of 4 m. An erosion model is developed for Monterey Bay where the erosion process is modelled as a non-linear function of the 4-m significant wave height

$$R = [AHs^2 + BHs + C(Tide + 1.02Hs - Clifftoe)]/Beach\ Slope$$

The coefficients A, B, C are computed from a least squares regression of the modelled and observed recession rate values. The erosion model provides a reasonable representation of the erosion process in Monterey Bay, where the mean standard error between observed and modeled erosion rates is ± 0.17 m/yr. Adjustment of the wave energy coefficient, A, allows tuning of the model for high and low wave energy locations.

TABLE OF CONTENTS

LIST OF TABLES

LIST OF FIGURES

ACKNOWLEDGEMENTS

I. EROSION PROCESSES IN MONTEREY BAY

A.   INTRODUCTION

Each year, the energy generated in vigorous Pacific storms is released upon the Monterey Bay coastline. As the massive, long period waves break in the surf zone, their power is transformed into the forces that drive littoral transport and coastal erosion. These two processes scour and transport hundreds of thousands of tons of sand annually within the Bay. The popularity of Monterey Bay has brought pressure to develop its coastline; yet, past developments in this energetic zone, without proper regard for the coastal dynamics, have resulted in grave economic consequences.

B.   BACKGROUND

Much of Monterey Bay area, particularly south of the Pajaro River, consists of low lying coastal plains bordered by foothills on the east, and active beaches on the west. This geomorphology is graphically depicted for South Santa Cruz County and North Monterey County in Figures 1.1, 1.2, and 1.3.   Centuries of sedimentary discharge from the San Lorenzo, Pajaro and Salinas Rivers have provided the abundance of sand required to build the coastal plains and beaches. This discharge, combined with a prevailing northwesterly breeze, and generally southerly longshore transport, has generated expansive sand dunes along the inshore side of the beach. In recent geologic time, however, the trend is towards erosion and not accretion. Erosion occurs when powerful storm waves, coupled with high tides, are able to rush up the foreshore and scour away at the base of the sand dunes. The undermining of the cliff causes the face of the dunes to collapse and fall onto the berm. Successive waves entrain the slumped sediment and carry it out into the littoral transport zone where it is either deposited into a less energetic region, lost into the Monterey Canyon, 726,800 m^3/yr, Oradiwe (1986), or mined by one of Monterey's three sand companies, which collectively mine on the order of 413,100 m^3/yr. Sand transport in Monterey Bay is shown in Figure 1.4.
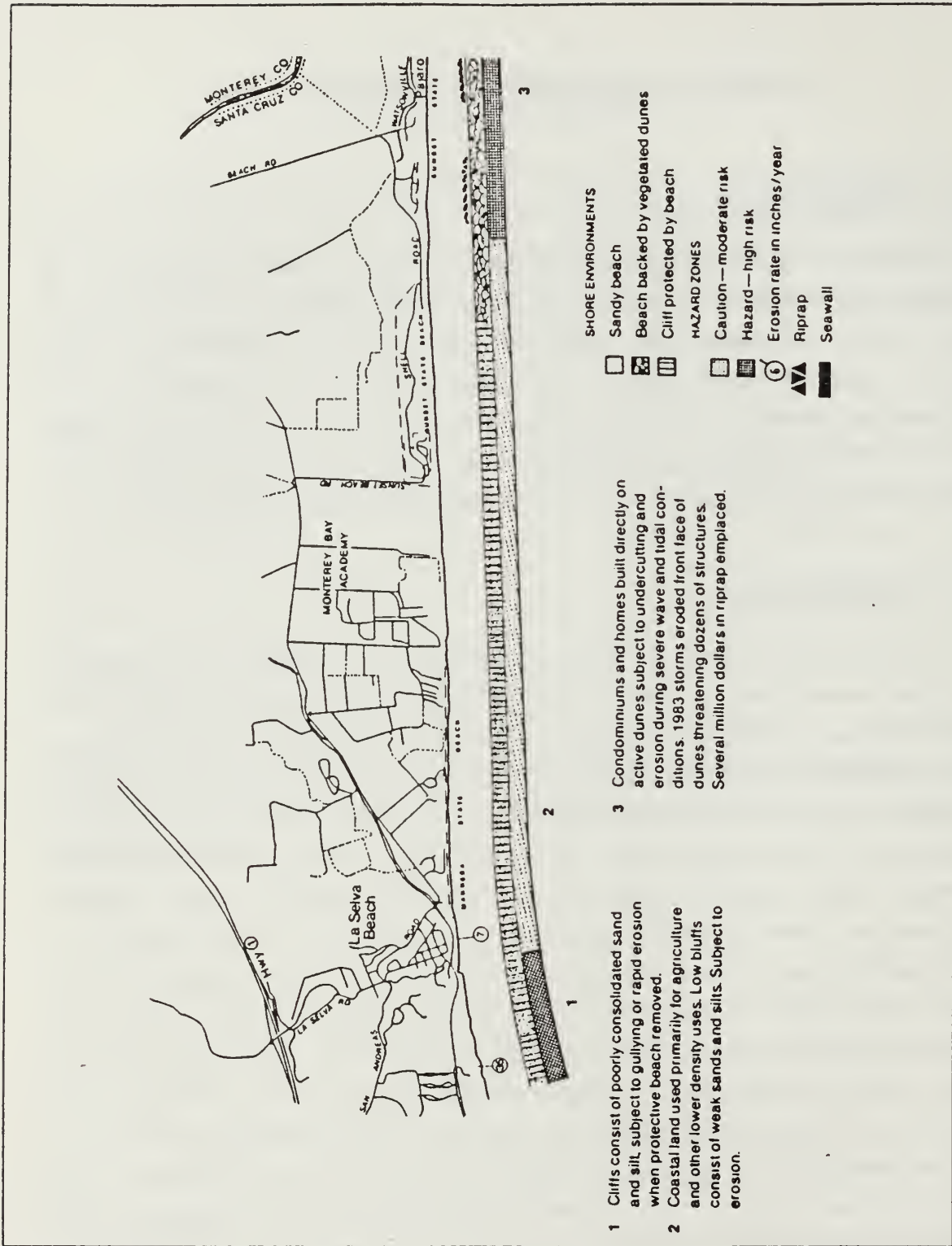
Figure 1.1   South Santa Cruz County (Griggs, 1985).
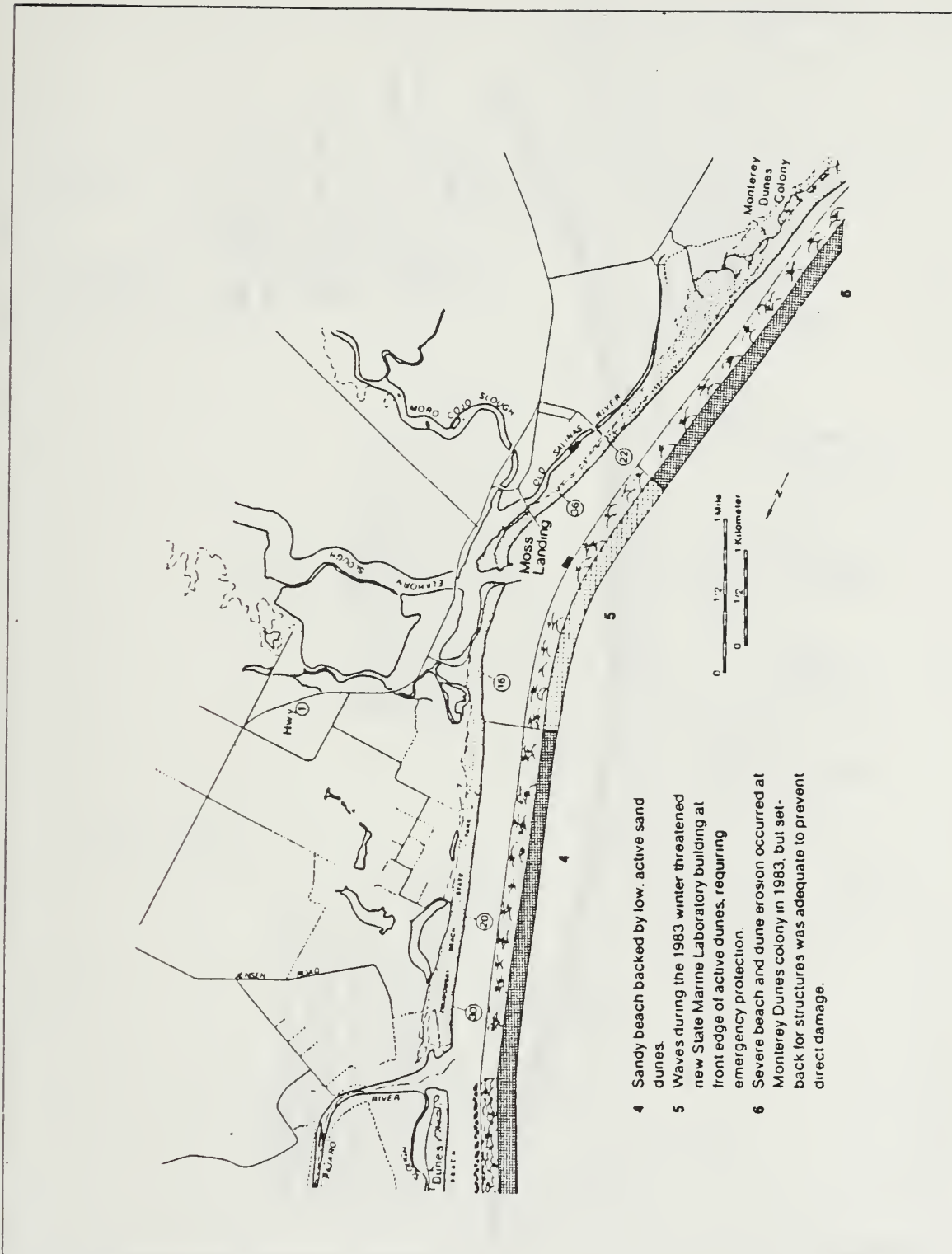
Figure 1.2   North Monterey County (Griggs, 1985).

11
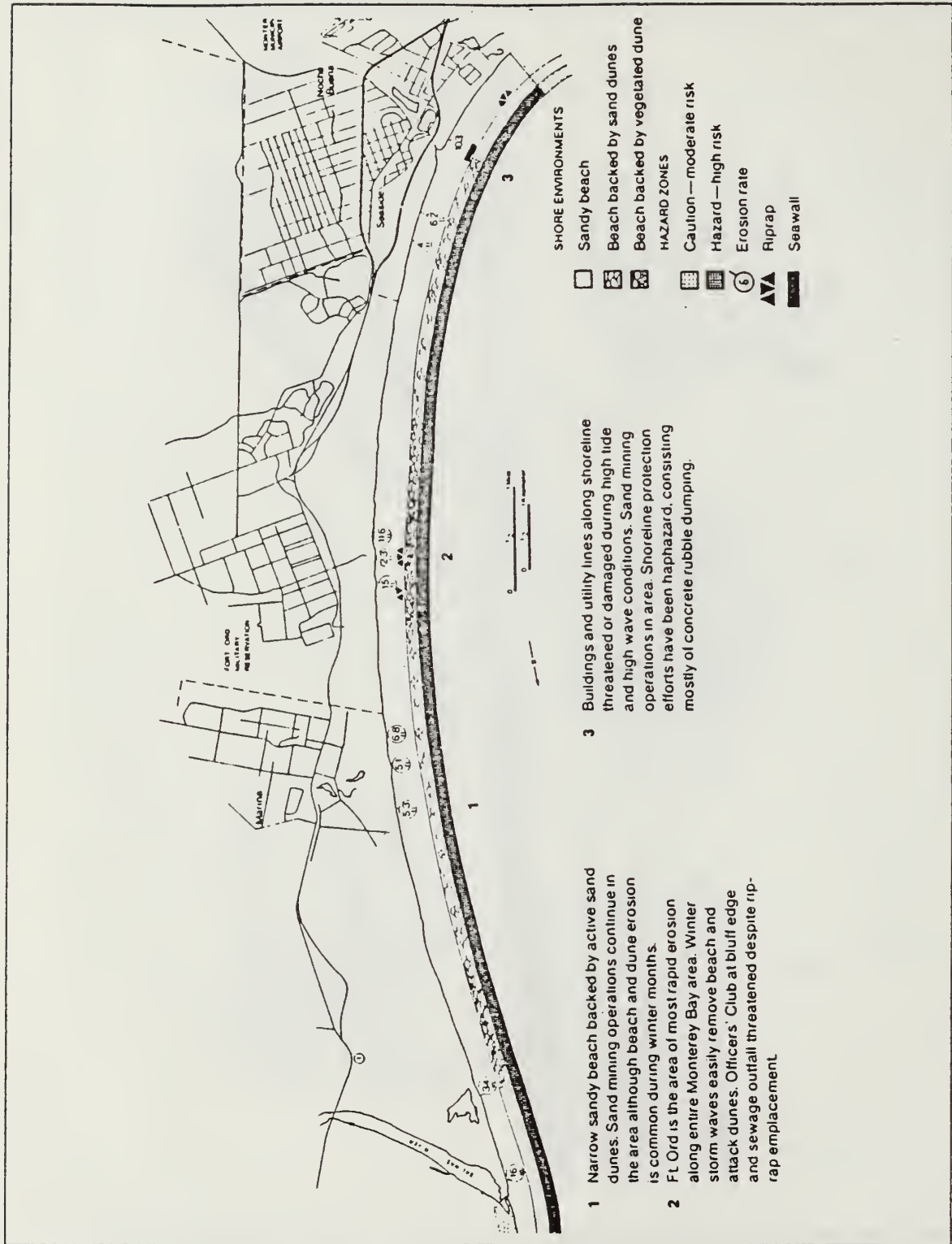
Figure 1.3 Central Monterey County (Griggs, 1985).
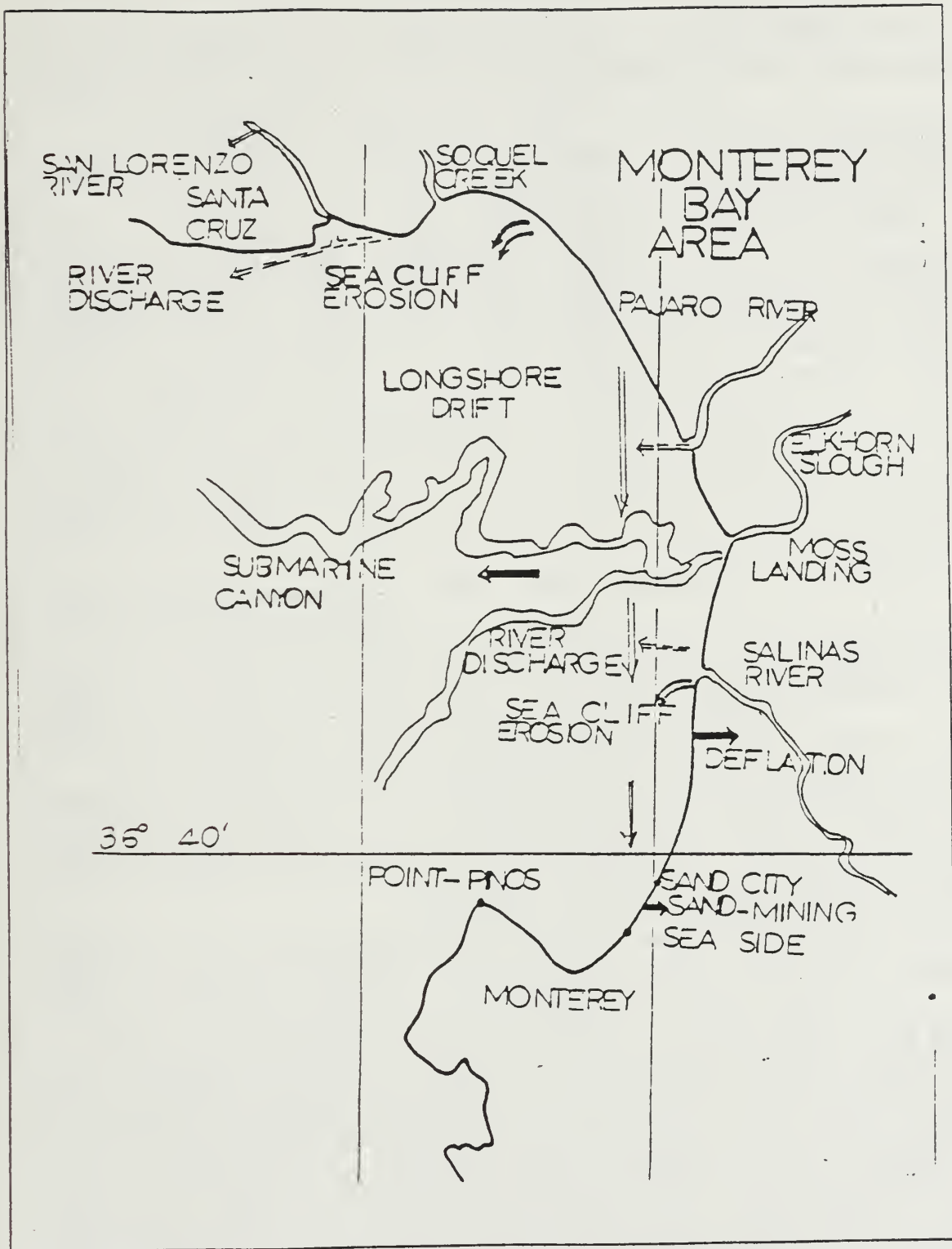
Figure 1.4 Littoral transport in Monterey Bay (Oradiwe, 1986).

C.   THE NEED FOR COASTAL EROSION DATA

The delightful climate and picturesque setting of Monterey and Santa Cruz Counties attract an ever expanding population. One manifestation of this population increase is mounting pressure to develop the coastal areas. Development of several areas along the Monterey Bay coastline without adequate knowledge of the coastal processes, has resulted in considerable monitary losses.

Seacliff State Beach, at the northern extreme of our research area, is a well documented example of a location that experiences storm damage with cyclic regularity. The seawall at Seacliff State Beach was destroyed and rebuilt three times between 1940 and 1978. In 1980 a new seawall was constructed at a cost of 1.7 million dollars. The structure was engineered to last twenty years, but unfortunately, in the winter of 1983, storm waves and their associated flotsam battered the structure until one third of the seawall was completely destroyed, and heavy damage was inflicted on many nearby camping facilities. The estimated reconstruction costs were $740,000. (Griggs, 1985)

Further south, the exclusive Pajaro Dunes condominium development was constructed in a region of active sand dunes. The development's location is one that experiences large scale episodic erosion followed by gradual accretion. The erosion occurs when the tidal stage is in phase with southwesterly storm waves. Three of these episodic erosion events occured between 1969 and 1983. The erosion was severe enough to cut the foredune back to the foundations of the development. Thousands of tons of riprap were placed in front of the development as a temporary measure during the 1983 storm season. The following summer, a permanent revetment fortress was built at a cost of several million dollars. (Griggs, 1985)

The Moss Landing Marine Laboratory was constructed on a site that has some interannual variability; however, accretion is the dominant morphologic process occuring on longer time scales. The foundation for the laboratory was laid in mid-December, 1983; yet less than one month later, storm waves cut back the foredune and encroached upon the construction site. Again, tons of riprap were implanted as a temporary measure, and a permanent seawall was installed the subsequent summer.

Perhaps the most dramatic and well documented case of episodic erosion has occurred at Stillwell Hall on the Fort Ord Military Reservation. Studies by Lima and Sklavidis (1984) found the average cliff recession rate to be 1.83 m/yr. This dramatic

erosion is consistent with the refractive focusing of wave energy to the area (Chapter III). The U.S. Army has recently spent $400,000 dollars as a temporary measure, while it contemplates whether to spend millions for permanent protection, move this soldier's recreation hall to a different site , or build a new one elsewhere.

Lima and Sklavidis (1984) used precise, non-automated photogrammetric techniques to establish erosion rates at four locations in southern Monterey Bay: NPS Beach Lab, Monterey Sand Company, Phillips Petroleum property, and Stillwell Hall. Their results for the Phillips Petroleum property strongly corroborated the results of Thompson (1981), and their method of inferring coastal erosion through bluff recession (Thornton et. al., 1985) minimized the variance in photogrammetric measurements.

Thompson (1981) viewed aerial photographs with a mirror steroscope to observe cliff toe recession at the Phillips Petroleum property in Monterey from 1939 to 1978. He concluded that the average recession rate was 0.6 m/yr. Moffitt (1968) used aerial photography to establish erosion rates in the vicinity of the Monterey Sand Company. Unfortunately, Moffitt referenced his data from the water line, the extreme variability of which resulted in rather large variance values. Nevertheless, he documented an average erosion rate of 2.1 m/yr.

Lima and Sklavidis (1984) found cliff recession rates of 1.5 to 2.7 m/yr along a mile stretch of Sand City beach on either side of the Monterey Sand Company. They attribute this locally high erosion rate to the sand mining operations.

The Monterey Beach Inn in Seaside and the Ocean House apartment complex in Monterey have both recently been threatened by major erosion events. The Monterey Beach Inn, previously named the Monterey Holiday Inn, constructed a permanent seawall to protect its investment, which at least thus far has been adequate. However, the Ocean House apartment management dumped five thousand tons of granite boulders onto the City beachfront adjacent to their complex as an emergency safegard measure. They are now required to remove the revetment from the public beach.

The recent erosion events in Southern Monterey Bay may be natural phenomena in the annual and interannual variability of the coastline; or, as has been suggested by Griggs (1985), the increased erosion may be a result of sand mining in the Southern Bay. The reduction of sand availability caused by mining operations may inhibit the ability of large sand bars to form offshore during the winter. The annual formation of the offshore bars acts as a natural buffer against the powerful winter storm waves. The big waves break on these offshore sand bars and a majority of their energy is dissipated

within the surf zone. Without the bars, or if they are reduced in size, energetic winter waves can expend their force directly on the beachface, and provide the energy required for a major erosion event.

The fact that several of the developed areas along Monterey Bay's coastline have suffered the severe consequences of building in the dynamic coastal zone should be taken as a forewarning. The increasing population of the Bay Area will bring more pressure to further develop this delicate area. It is clear that quantifiable erosion rate data and wave climatology must play a key role in site selection and structure engineering in order to prevent the inevitable destruction of improperly situated, or engineered sites.

D.   OBJECTIVES

The objective of this thesis is to develop a predictive model for coastal erosion in Monterey Bay. Erosion rates are inferred from bluff recession, which is measured using precise digital photogrammetric techniques from a 44-yr time series of aerial photographs. Reference points that define the beach profile must be chosen to insure both sharp definition of the reference on an aerial photograph, and accurate depiction of permanent, long-term erosion. The variability of the foreshore profile caused by seasonal sediment transport renders it unsuitable as a measurement reference. Similarily, cliff material that has fallen onto the cliff toe makes that potential reference difficult to define, and generally unreliable. The sharp stereo presentation of the cliff top however, offers an ideal profile, and one that is not subject to short time-scale variability. Consequently, changes in the cliff top profile reflect permanent recession. Twelve sites have been chosen from Monterey, north to La Selva Beach and bluff recession is measured along 400-to 1300-m coastal intervals centered on each of the twelve sites. The resultant erosion rate data is used along with a 20-yr spectral wave climatology and tidal information in the development of a coastal erosion model.

A majority of the previous erosion studies that led to quantifiable results used imprecise methodology in photographic measurement. These inadequate procedures produced questionable results and unquantifiable errors. The precise photogrammetric technique used by Lima and Sklavidis (1984) produced results with acceptable confidence limits. The manual mode of the stereocomparator that they used, however, induced operator measurement errors (reading the vernier), and was extremely time consuming. Hence only four sites were completed.

16

Our research employs digital equipment and techniques to minimize and make it easier to quantify operator and position measurement error. The variance in bluff recession data is minimized through numerical integration of the chosen coastal segments, and a comprehensive survey of the twelve coastal sites insures that the model will be representative of the erosion processes in Monterey Bay.

II. PHOTOGRAMMETRY

A.   BACKGROUND

Precise photogrammetry is the currently recognized and practiced cartographic method of producing accurate, cost effective, topographic maps and shoreline manuscripts for nautical charts. Its accuracy for measuring events occuring on long time scales, such as cliff recession, is far superior to the previously employed methods of inferring coastal erosion through comparison of historical maps and charts, or subjective "hand" measurements on aerial photographs.

This research uses planimetric and precise metric photogrammetric techniques to establish cliff recession rates. Planimetric photogrammetry is employed to qualitatively survey the selected measurement sites. At this initial stage, the photogrammetrist views the photo model stereoscopically to select the scaling points, identify local photo control points, determine the clarity of the cliff line, and establish the overall servicability of the photographs. Once these points have been identified, a field survey is performed to obtain the ground distance between scaling points, the height of the berm, and the elevation of the cliff top (above MLLW). Accurate quantitative measurements are then made using a precise stereocomparator.

B.   SITE SELECTION

In any erosion study, it is advantageous to establish the erosion rates for the entire coastal survey area; unfortunately, the use of such a method on large scale erosion problems becomes economically unfeasible. A viable alternative, however, is to choose a number of study sites in the survey area that are representative of the overall erosion processes. This thesis examines twelve sites in Monterey Bay from the City of Monterey north to La Selva beach. Erosion information has been calculated for eight of the twelve sites examined, and results from Lima and Sklavidis (1984) are used for the remaining four sites. The specific criteria for site selection are listed below:

*   Is the site of economic interest ?
*   Is the site of scientific interest ?

* Is the site of political interest ?
* Does the site lend itself to the use of photogrammetric techniques ?
* Will the site provide representative erosion rates ?

The total number of sites had to be limited to what was felt could be accomplished within the given time constraints. Additionally, the sites had to be spaced along the Bay's coastline in such a manner as to provide representative coverage, and all sites had to be photogrammetrically usable. The geographic positions of each of the sites and their associated names are provided in table I. The actual study area consisted of a 500-to 1300-m stretch of bluff in front of each site. The site locations are shown in Figure 2.1.

C. POTENTIAL ERRORS ASSOCIATED WITH PHOTOGRAMMETRY

The primary sources of error in photogrammetric data are caused by image displacement and scale variation. Specifically, photogrammetric errors can be classified into three basic catagories: relief displacement, tilt displacement, or terrain induced scale variations.

Relief displacement in a vertical photograph occurs when an image is displaced from its actual position due to an elevation difference between the image and the photographic principal point. Images of points on photographs with significant topographic relief will be displaced radially outward and images at lower elevations radially inward from the photographic principal point, as shown in figure 2.2. Displacement has the effect of portraying distances between images at higher elevations to be greater than they actually are, and distances between images at lower elevations to be less than they actually are. Relief displacement can be quantified and is given by

$$d = (r \times h)/ H \qquad\qquad (2.1)$$

where d is the radial displacement distance, r is the radial distance from the principal point to the image, h is the image elevation above datum, and H is the flying height.

Tilt displacement occurs when an image is displaced from its actual position resulting from a tilt in the vertical camera angle at the time of photo exposure. On a vertical photograph, thè nadir, n, and the principal point, o, are indeed the same point.

TABLE I
SELECTED SURVEY SITES

Station Name	Latitude	Longitude
NPS Beach Lab	36°36'10" N	121°52'25" W
Phillips Petroleum	36°36'36" N	121°51'50" W
Sand City	36°37'00" N	121°51'15" W
Monterey Sand Co.	36°37'20" N	121°50'55" W
South Fort Ord	36°38'05" N	121°49'55" W
Stillwell Hall	36°39'40" N	121°49'17" W
Marina	36°41'58" N	121°48'32" W
Rincon Beach	36°46'30" N	121°47'48" W
Marine Lab	36°47'35" N	121°47'32" W
North Moss	36°48'25" N	121°47'25" W
Zmudowski Dunes	36°49'40" N	121°47'50" W
Monterey Bay Academy	36°54'26" N	121°50'55" W

However, when a camera is tilted at the time of exposure, its bore sight will describe the photograph's principal point, and a plumb line from the camera's optical center will describe its nadir, obviously now, not the same point. This distinction is important because image displacement on a tilted photograph will occur along radials of the nadir point, and not the principal point as was the case with relief displacement. Photographs with tilt displacement can be rectified by projecting their coordinates onto a new plane that is parallel to the map plane, or datum. The coordinates projected onto the new plane then comprise the equivalent vertical photograph. Tilt information was available for all of the photographs selected for this research, and only photographs with less than three degrees of tilt were used to establish cliff recession rates. The image displacement resulting from a $3°$ tilt of the horizontal flight line axis is less than the photocomparator's resolution ability; thus, all photographs employed in this thesis were considered vertical. The geometry of tilt displacement is given in Figure 2.3.

Terrain-induced scale variation is another effect of vertical relief on a two-dimensional photograph. A manifestation of scale variation is that higher elevations will appear on the photograph at larger scales and lower elevations will appear at smaller scales (assuming a constant flying height). This variation is shown in Figure 2.4. In a photogrammetric mission, scale variation can be decreased by increasing the flying height and camera focal length.

There are two procedures for minimizing the effect of the aforementioned errors in a photogrammetric data base. The first procedure is to apply point specific tilt, relief, and scale correctors to each measurement taken on the photograph. Unfortunately, hundreds of measurements are typically taken on each photograph, and this process is slow and laborious. The second procedure, and the method adopted by this research, is to choose ground control, and scaling points that are both, as close as possible to the measurement region, and at nearly the same elevation. Proper choice of the control and scaling points insures that the photogrammetric measurements are made over distances close to the baseline, and that the photoscale is highly accurate for the measurement region. Photoscale is given by

$$S = (ab)/(AB) \tag{2.2}$$
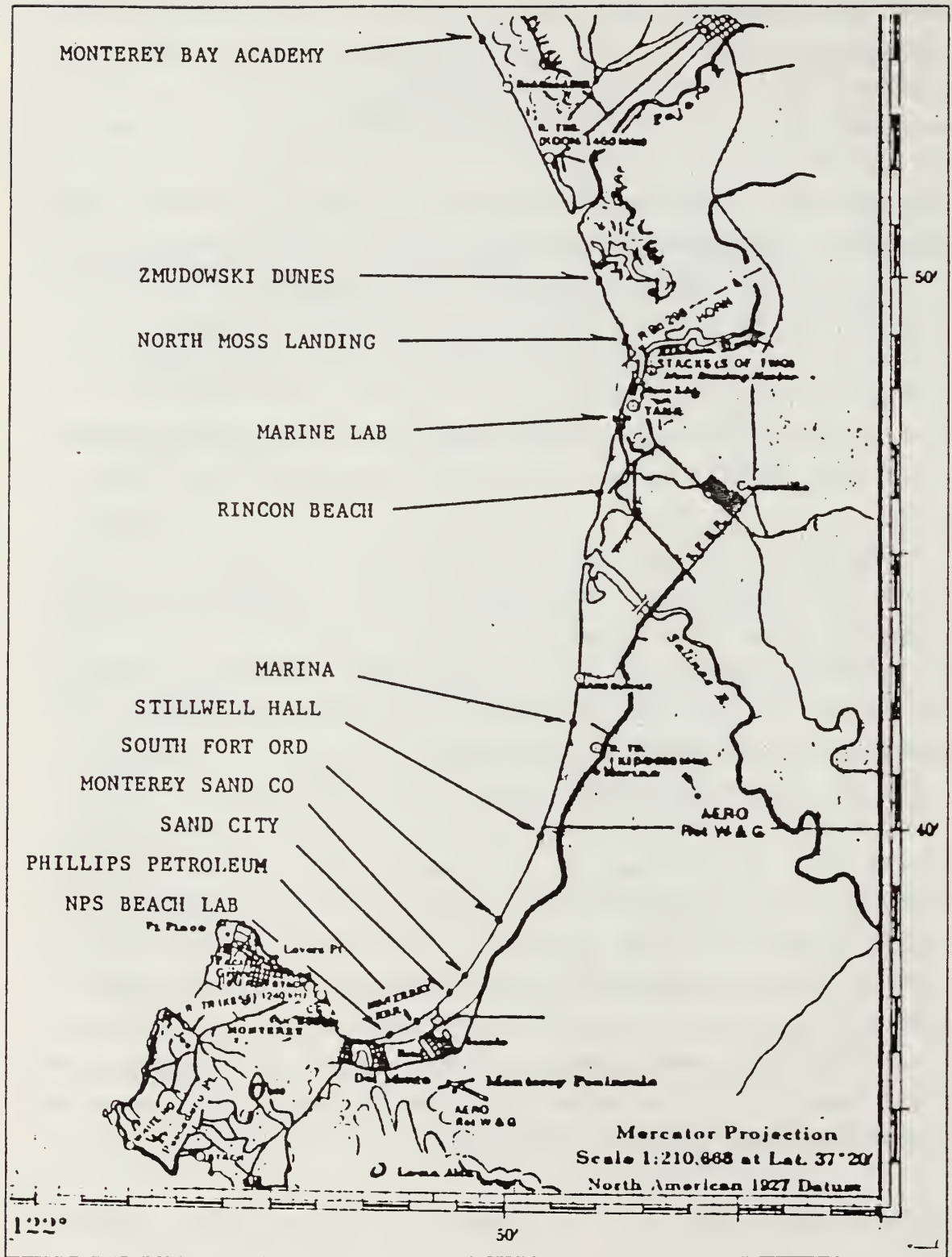
Figure 2.1   Erosion Rate Evaluation Sites.
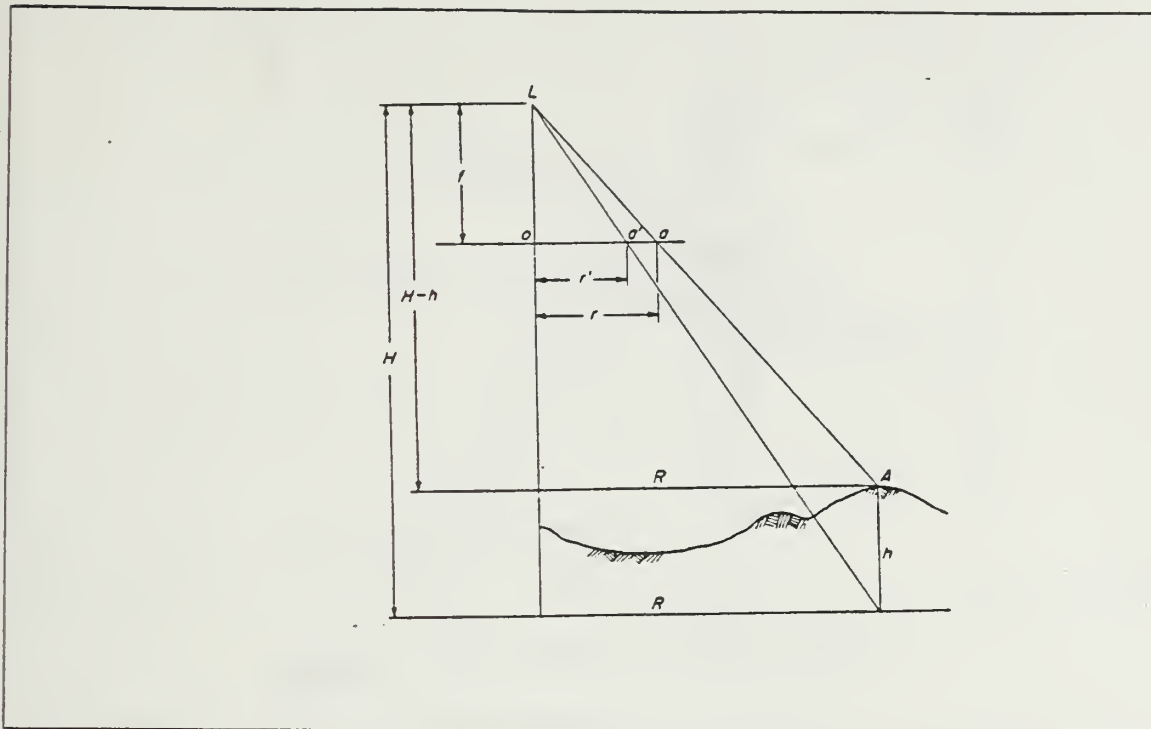
Figure 2.2   Relief Displacement (Moffitt, 1980).

where AB is the measured ground distance from the field survey, and ab is the photodistance measured with a photocomparator. A more detailed discussion of photogrammetric errors and their correctors can be found in Moffitt (1980).

D.   INSTRUMENT ACCURACY AND SET UP

Photogrammetric measurements were made on a modified Zeiss stereocomparator interfaced to an IBM Personal Computer (IBM-PC). A schematic of the Zeiss instrument is provided in Figure 2.5. The digital modification was accomplished by placing Teledyne-Gurley DMC-400 encoders on the stereocomparator's X, Y, and X-parallax adjustment controls. Each encoder outputs 8000 counts per one revolution of the comparator's controlling screws. Horizontal coordinates can be read from the instrument's verniers to an accuracy of 0.01 mm, and the X - parallax control can be read to 0.001 mm (Hallert, 1960). For calibration, numerous readings were taken along each of the instrument's three verniers, and paired with their associated encoder counts. A linear regression was then performed for each of the three paired data sets

23
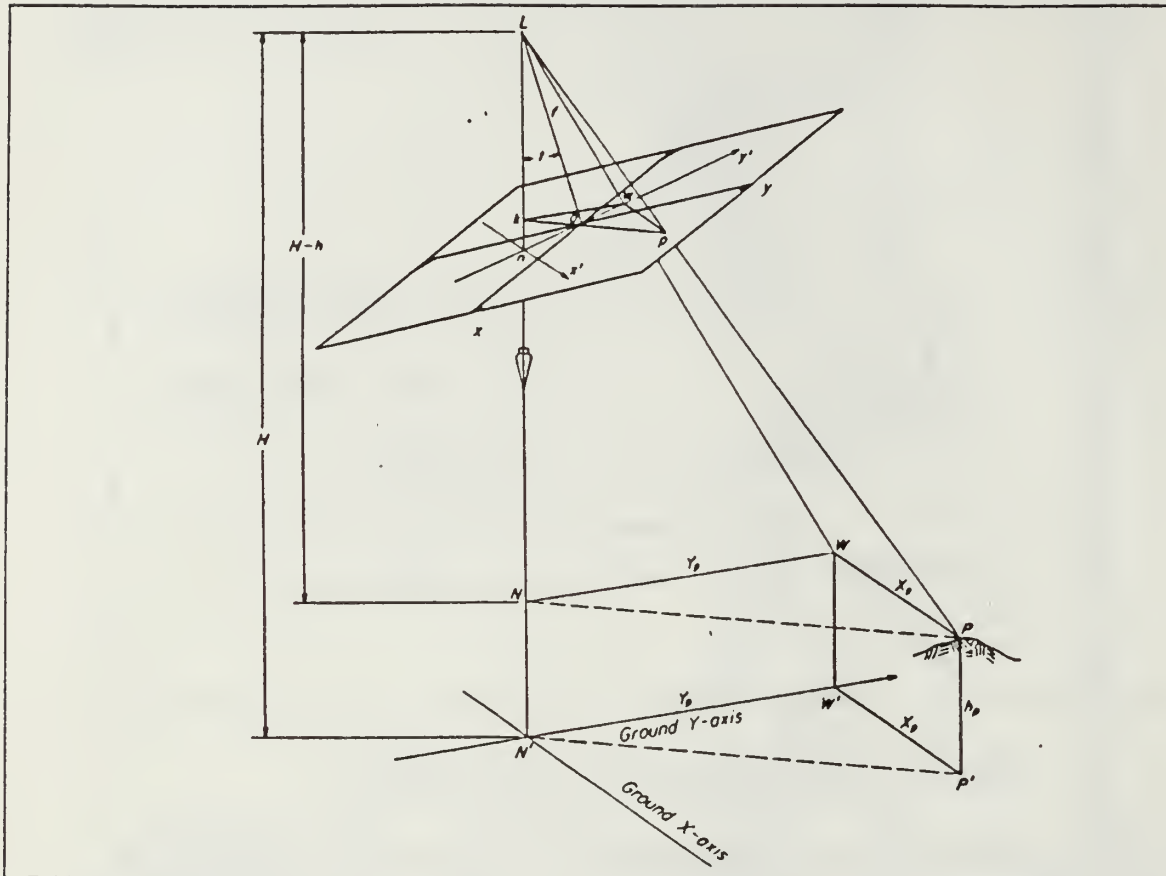
Figure 2.3   Tilt Displacement (Moffitt, 1980).

to provide encoder count to horizontal distance transfer functions. These functions were evaluated for uncertainty by first calculating the standard deviation, or standard error for each axis, which were found to be: $\sigma_x = 0.009$ mm, $\sigma_y = 0.024$ mm. The RMS radius of the error circle, or position error, d_r , for an uncorrelated, orthogonal coordinate system is given by Heinzen (1980) as

$$d_r = (\sigma^2_x + \sigma^2_y)^1/2 \qquad\qquad (2.3)$$

and is found to be 0.022 mm . This photo position error can be converted to ground position error by multiplying d_r by the photoscale. For example, the ground position error on a 1:12,000 scale photograph would be two tenths of a meter.

Stereo vision presents the sharpest possible presentation of the standard 9″ × 9″ photographic data. A pair of overlapping photographs are placed on plates 1 and 2 of

24
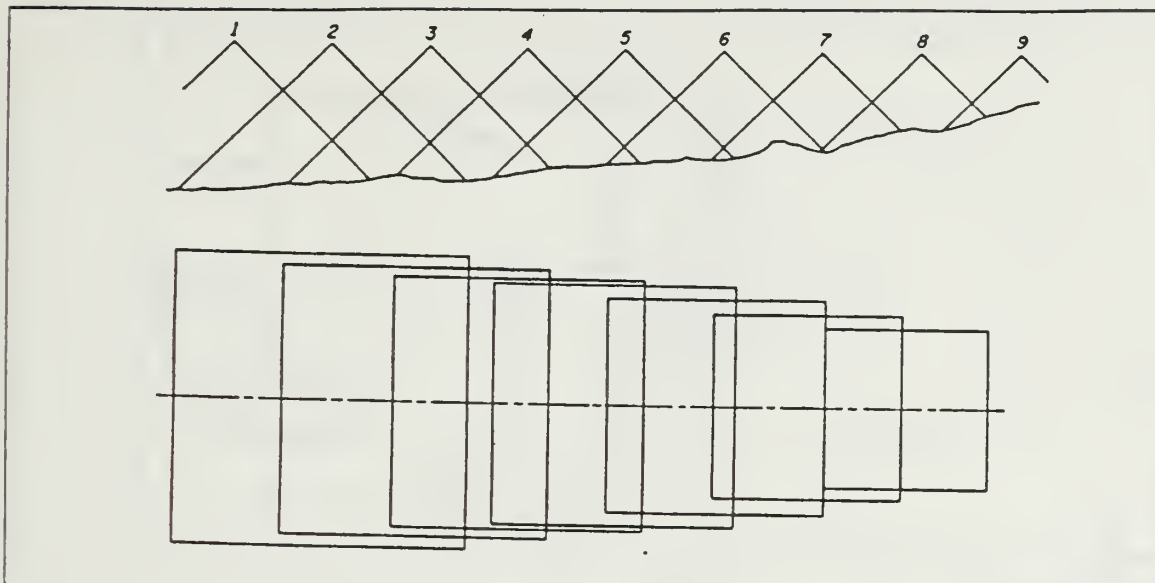
Figure 2.4   Scale Variation (Moffitt, 1980).

the photocomparator (Fig. 2.5), each of which may be rotated in a plane normal to the vertical axis of the photograph. The image on plate 1 is rotated until the X-fiducials are parallel to the flight line (X-axis of the photocomparator). The image on plate 2 is also rotated to align the X-fiducials with the flight path, but additionally, a Y-parallax adjustment must be made to bring the flight line on image 2 into coincidence with the flight line on image 1. The Y-parallax will have been completely removed once the two flight lines are in coincidence, and the operator will be able to see two marks in the stereo viewer. One mark, on image 1, will be stationary, the other mark will appear to float above the photograph (Figure 2.6). The X-parallax or elevation, control is then adjusted until the floating mark becomes coincident with the fixed mark. The conjugate points on the two photagraphs are now viewed as exactly the same point and precise stereo measurements can be made.

E.   MEASUREMENT PROCEDURE

Several points are selected that appear on each stero model in a particular photographic time series. These points are: a coordinate system origin, O; a baseline definition point, B; and numerical integration limits, L_l and L_u (Figure 2.7). Annual and interannual variability of the sand dunes render it impossible to repeatedly locate

25
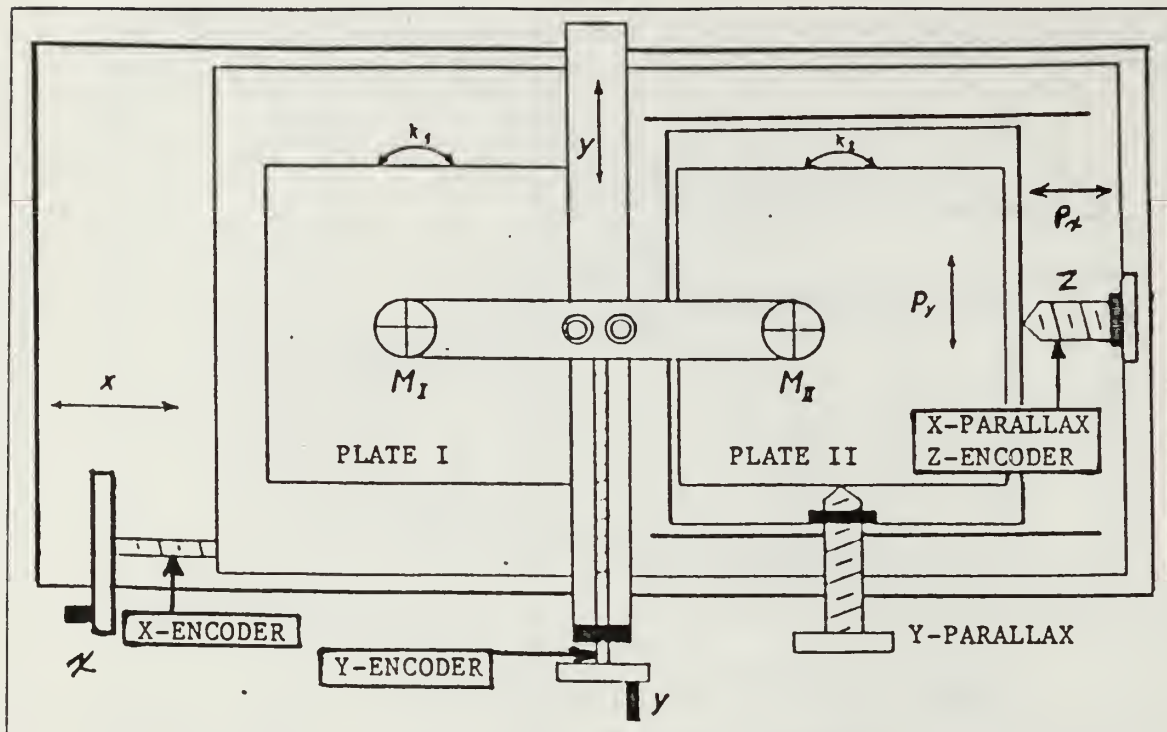
Figure 2.5   Zeiss Sterophotocomparator.

the integration limits by sight on a photograph; instead, these points are accurately located by the intersection of the cliff edge and a line normal to the cliff that has been defined by two reliable points, IP_1 and IP_2 discernable on the photographs. The same scaling points are typically selected for each stereo model. This procedure is not always possible, however, and additional scaling points sometimes have to be chosen. Such additional points must be supported by supplimental field work.

Digital coordinates are obtained through employment of an interactive program which is designed to communicate between the comparator's encoders and the IBM-PC. The program, PHOTODAT, accepts commands from the IBM-PC keyboard and writes the desired coordinates into a station data file. PHOTODAT is listed in Appendix A. The digital data acquisition procedure is very specific and requires the origin of the photographic coordinate system be defined first. This step is accomplished by moving the comparator mark to the designated position, O, and entering it. The operator must then move the mark to the baseline definition point, B, and enter its position. The X and Y values of point B define the coordinate system rotation angle α given by
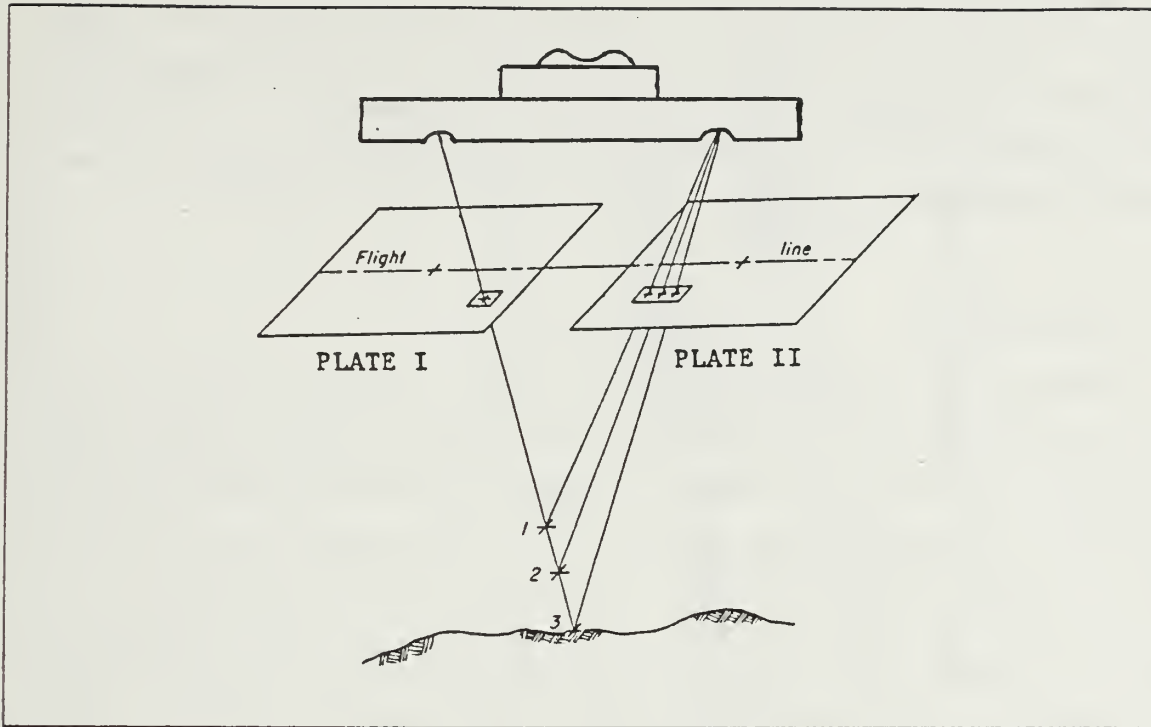
Figure 2.6   X-Parallax and the Floating Mark.

$$\alpha = \arctan(Y/X) \tag{2.4}$$

All points entered subsequent to the baseline definition point are projected onto a new coordinate system via the coordinate system rotation matrix

$$\begin{bmatrix} X^1 \\ Y^1 \end{bmatrix} = \begin{bmatrix} \cos\alpha & \sin\alpha \\ -\sin\alpha & \cos\alpha \end{bmatrix} \times \begin{bmatrix} X \\ Y \end{bmatrix} \tag{2.5}$$

The scaling parameters are the next points entered, and the first points to be projected onto the new coordinate system. Once the photographic scale has been accurately defined, bluff measurenents can begin. The cliff edge is outlined by a dense network of points entered monotonically along the cliff from point L_l to L_u. The actual cliff outline is approximatcd by line segments whose lengths vary slightly with topography but are typically less than 0.25 mm at photoscale. A trapazoidal rule integration was performed to determine the area between the cliff edge and the baseline using

$$\sum_{i=1}^{N} [(Y_i + Y_{i+1})/2 \times |X_{i+1} - X_i|] \tag{2.6}$$

27

Areas for adjacent years in the time series were subtracted to provide the actual eroded area, and that figure was multiplied by the mean cliff elevation to determine the eroded volume. The actual coordinate system rotation, scaling, and numerical integration are performed by an interactive program, WRKPROG (Appendix B). WRKPROG retrieves raw data from the PHOTODAT files, accepts inputs from field surveys, and executes the numerical computations.

F.   FIELD SURVEY

A separate field survey was performed for each of the eight erosion sites. One task of the field party was to determine the authenticity of the photo control and scaling points. If there was any doubt as to whether a particular reference point had been moved or changed sometime during the 44-year photographic time series, that point was rejected, and another selected. Additionally, accurate distances had to be measured between the ground scaling points to determine the precise photographic scale. This operation was accomplished using a Keuffel and Esser, Ranger-IV, laser distance measuring device. The K&E Ranger-IV has an accuracy of ± 5 mm + 2 ppm (Keuffel and Esser, 1975). At typical measurement distances of 800 m, this uncertainty translates to $\pm 5 \times 10^{-4}$ mm on a 1:12,000 scale photograph. A standard deviation of $\pm 5 \times 10^{-4}$ mm is one full order of magnitude less than the Zeiss photocomparator's resolving power; consequently, no accuracy was sacrificed through use of the Ranger-IV. The scaling distances at each station were measured ten times and averaged to insure the best possible results. Temperature, pressure and humidity were observed at each measurement site, and the measured distance was corrected for atmospheric refraction effects.

The elevation of the cliff toe was measured at 75-m intervals along each site's beachfront. The elevation measurement was observed using a surveyor's level and a Philadelphia rod. The actual cliff toe elevation was leveled from the mean water line, and the measurements were subsequently reduced to datum (MLLW) using tidal correctors.
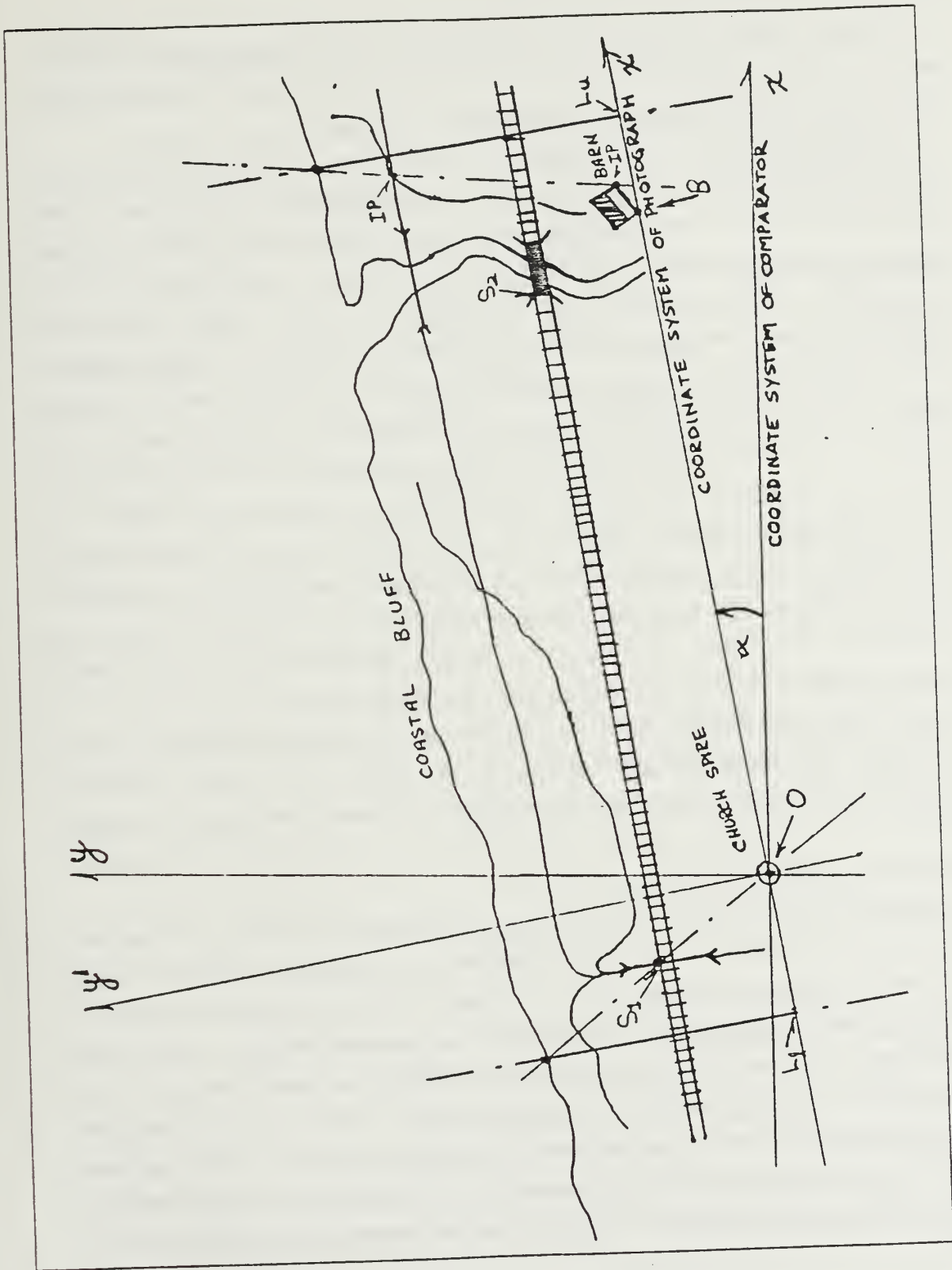
28

Figure 2.7   Photo Measurement Technique.

29

G. EROSION DATA PRESENTATION

Erosion results are presented for eight sites along Monterey Bay: Sand City, South Fort Ord, Marina, Rincon Beach, Moss Landing Marine Lab, North Moss Landing, Zmudowski Dunes, and Monterey Bay Academy.

Typically, 75 to 150 points are digitized from each stereo model. Integrated areas for adjacent photo models in the time series are subtracted, and the difference is the recessed area for the intervening time period. The recessed area is divided by the longshore observation distance (length of the digitized bluff), and that value is divided by the number of years between the photo models. The result is a cliff recession rate in meters per year. Negative values in the tables below indicate recession, whereas positive values indicate accretion. A standard deviation is calculated for the recession rates at each site, and that value is stated in the respective site's result table. The number of standard deviations by which a particular recession rate drifts away from the mean value is listed in the tables' $"|x_i - \bar{x}|/\sigma "$ columnns, and provides a measure of temporal variability. Assuming episodic recession, a high value in the sigma column would signal an erosion event; however, it is important to also consider the length of the intervening time period. Long time intervals will tend to alias erosion events, and conversely, erosion events occuring within a short time period will be highlighted. Average erosion is inferred by multiplying the recession rate by the average cliff elevation. Not surprisingly, areas of refractive wave focusing resulting in energy convergence experienced the highest recession rates; whereas sites located at the head of Monterey Canyon, where there is refractive divergence, experienced long-term accretion. It is noteworthy that all sites experienced at least one significant erosion event between 1980 and 1984.

Sand City is a site that does not have a well defined coastal bluff. The bluff was approximated by digitizing the crest of the seaward-most sand dune. While recession is the dominate process occurring over the 44-year time series, significant accretion occurred between 1940 and 1956. This point is interresting, because - whether this growth event was a manifestation of sand dune variability, or bonifide accretion - the process made an abrupt change late in the time period. In the years following 1966 Sand City displayed recession rates comparable to those of Fort Ord, where high wave energy drives the highest recession rates recorded in Monterey Bay. The high recession rates observed at Sand City are not corroborated by the wave energy studies discussed

in Chapter III. The recession results at Sand City most likely reflect the presence of the sand mining industry which is most prevalent in that region of the Bay (Table II and Figure 2.8).

The highest recession rates we observed were at South Fort Ord. The recession is depicted in Table III and Figure 2.9, where the average bluff receded fifty meters from 1940 to 1984. This high rate is consistent with the refractive wave energy focusing which appears to be a maximum in this region.

Marina is also a site where high wave energy produces high recession rates. Additionally, numerous observations suggest that Marina is an area of high wind energy, perhaps due to geographic focusing of the seabreeze. The high wind energy and the variable nature of the non-solidified coastal bluff cause high variance in the observed recession rates, and may, in part, be responsible for the anomolous accretion observation in the 1970 time frame (Table IV and Figure 2.10).

Station Rincon Beach at the northern "edge" of the South Bay's energy convergence zone displays continuous recession from 1940 to 1984. The inference of a convergence zone boundary is made as wave energy increases south of Rincon Beach, and stations just north of Rincon exhibit long-term accretion. The recession at Rincon Beach is seen in Table V and Figure 2.11.

Accretion at station Marine Lab is evidenced by a shift in the entrance of Elkhorn Slough which occurred sometime between 1940 and 1966. This shift is clearly depicted in Figure 2.12. Figure 2.13 omits the slough entrance to present the recession/accretion events as they occurred after 1966. The numerical values are seen in Table VI.

The low wave energy caused by refractive divergence at the head of Monterey Canyon is responsible for littoral deposition and the resultant accretion at station North Moss Landing (Table VII and Figure 2.14).

Station Zmudowski Dunes appears to be the northern conjugate of Rincon Beach. It is a location where higher wave energy produces continuous recession, yet only 1.5 miles to the south, lower wave energy allows the accretion process to dominate at station North Moss Landing. Figure 2.15 graphically depicts the recession, and the recession rates are provided in Table VIII. The variability of McClusky Slough is evident in figure 2.15 and is omitted to present Figure 2.16.

Recession is the dominate process occurring at Monterey Bay Academy between 1956 and 1984. The wave energy focused to the north of Monterey Canyon is typically

31

not as high as energy which has been focused to the south. This point is almost intuitive, as a majority of the winter swells originate from extratropical cyclones in the Gulf of Alaska. Accordingly, the recession rates at Monterey Bay Academy are less than those at its southern conjugate station South Fort Ord. The recession at Monterey Bay Academy is presented in Table IX and Figure 2.17.

TABLE II
EROSION RATE RESULTS FOR SAND CITY

STATION NAME : Sand City

LATITUDE : 36°37'00" N

LONGITUDE : 121°51'15" W

MEAN CLIFF TOE ELEVATION (above MLLW) : 4.53 M.

MEAN CLIFF TOP ELEVATION (above MLLW) : 10.04 M.

LONGSHORE OBSERVATION DISTANCE : 540.00 M.

BEACH SLOPE : 1:40.00

SIGMA : 1.00 M.

TIME INTERVAL	RECESSION [M/YR]	$\frac{\|x_i - \bar{x}\|}{\sigma}$	AVG. EROSION [(M^3/YR)/M]
1940 - 1956	+ 0.47	1.44	+ 4.72
1956 - 1970	-2.30	1.33	-23.09
1970 - 1976	-1.22	0.25	-12.25
1980 - 1984	-1.34	0.37	-13.45
1940 - 1984	-0.97	......	-9.74
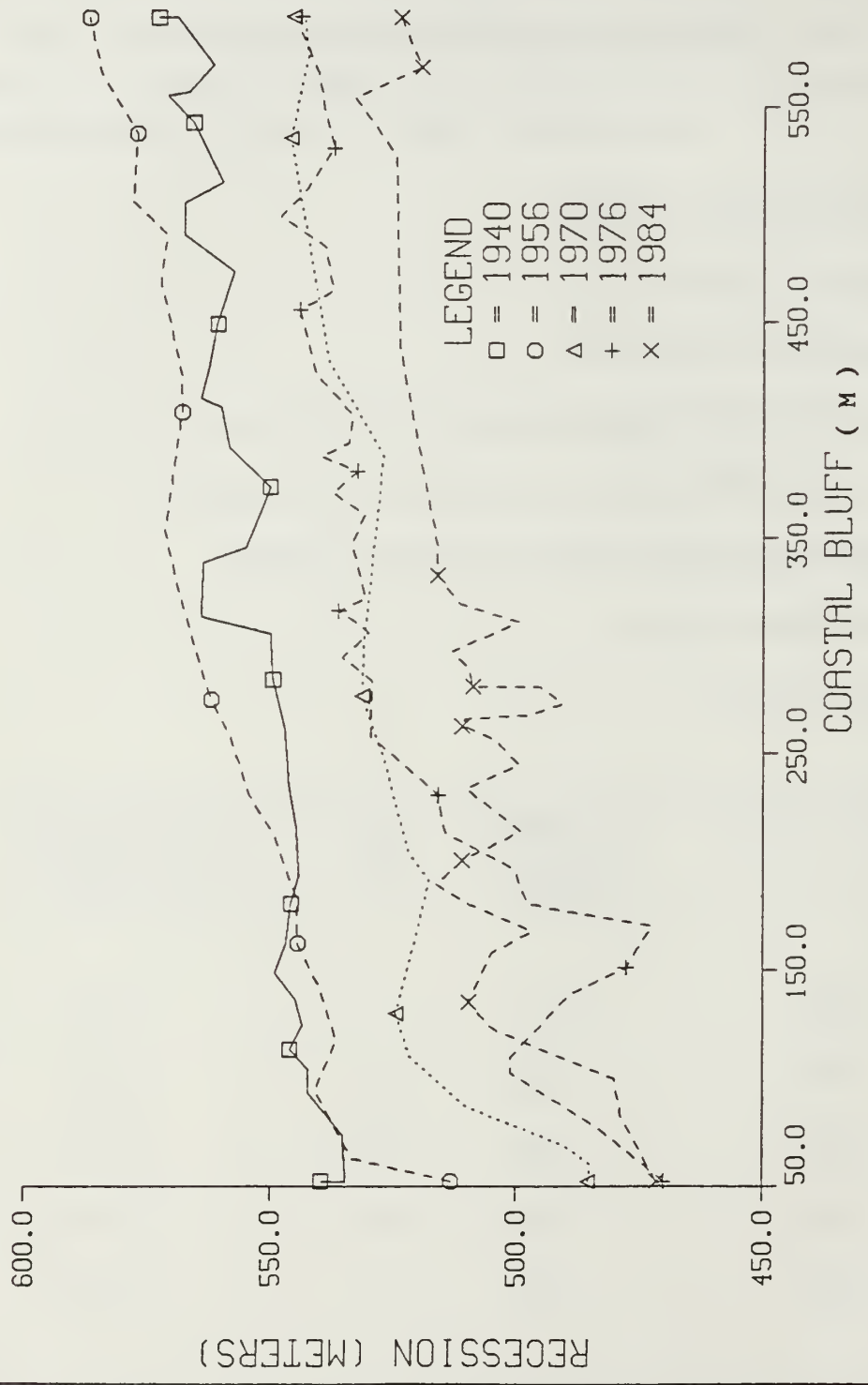
Figure 2.8   Sand City Erosion Results.

TABLE III
EROSION RATE RESULTS FOR SOUTH FORT ORD

STATION NAME : South Fort Ord

LATITUDE : 36°38′05″ N

LONGITUDE : 121°49′55″ W

MEAN CLIFF TOE ELEVATION (above MLLW) : 6.19 M.

MEAN CLIFF TOP ELEVATION (above MLLW) : 35.39 M.

LONGSHORE OBSERVATION DISTANCE : 692.00 M.

BEACH SLOPE : 1:36.36

SIGMA : 1.47 M

TIME INTERVAL	RECESSION [M/YR]	$\frac{|x_i - \bar{x}|}{\sigma}$	AVG. EROSION [(M^3/YR)/M]
1940 - 1956	-1.09	0.02	-38.58
1956 - 1966	-0.01	0.75	-0.35
1966 - 1980	-1.13	0.01	-39.99
1980 - 1984	-3.85	1.86	-136.85
1940 - 1984	-1.12	......	-39.64
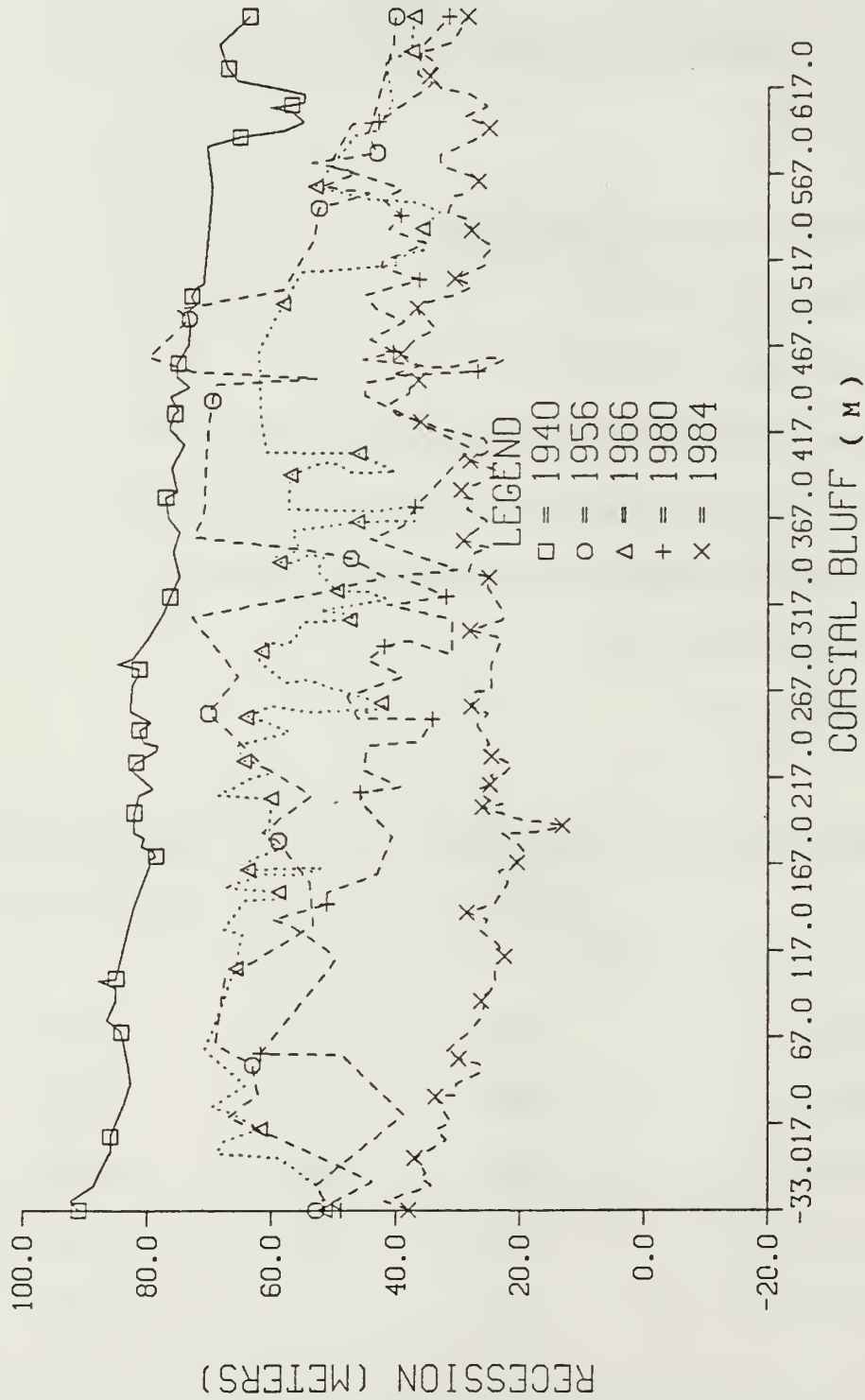
Figure 2.9   South Fort Ord Erosion Results.

TABLE IV
EROSION RATE RESULTS FOR MARINA

STATION NAME : Marina

LATITUDE : 36°41'58" N

LONGITUDE : 121°48'32" W

MEAN CLIFF TOE ELEVATION (above MLLW) : 4.92 M.

MEAN CLIFF TOP ELEVATION (above MLLW) : 24.31 M.

LONGSHORE OBSERVATION DISTANCE : 1283.00 M.

BEACH SLOPE : 1:40.00

SIGMA : 1.67 M.

TIME INTERVAL	RECESSION [M/YR]	$\dfrac{\|x_i - \bar{x}\|}{\sigma}$	AVG. EROSION [(M³/YR)/M]
1940 - 1956	-0.99	0.36	-14.83
1956 - 1970	-1.12	0.44	-27.23
1970 - 1980	+2.30	1.60	+55.91
1980 - 1984	-2.12	1.05	-51.54
1940 - 1984	-0.38	......	-9.24
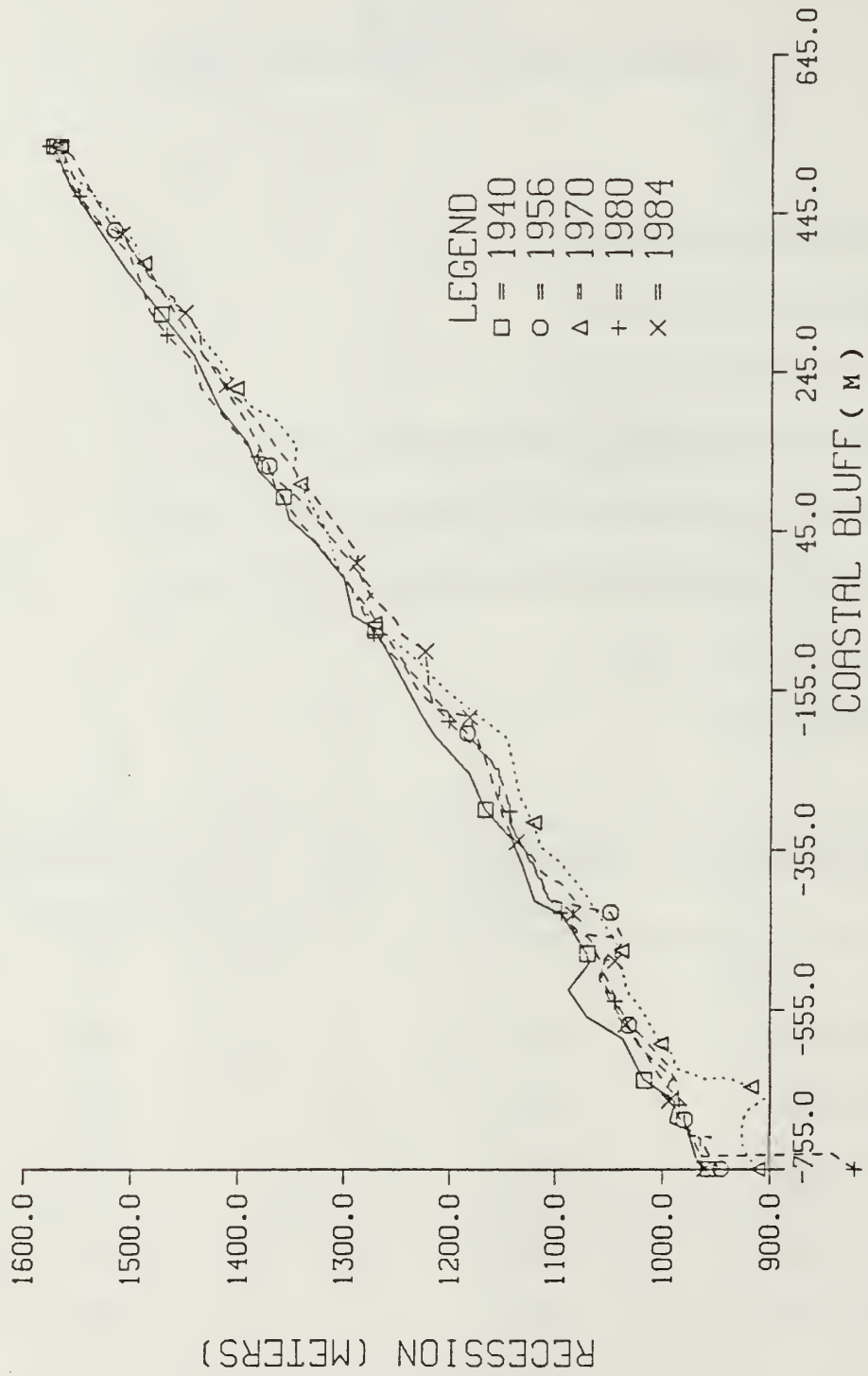
Figure 2.10   Marina Erosion Results.

38

TABLE V
EROSION RATE RESULTS FOR RINCON BEACH

STATION NAME : Rincon Beach

LATITUDE : 36°46′30″ N

LONGITUDE : 121°47′48″ W

MEAN CLIFF TOE ELEVATION (above MLLW) : 5.33 M.

MEAN CLIFF TOP ELEVATION (above MLLW) : 8.41 M.

LONGSHORE OBSERVATION DISTANCE : 1353.00 M.

BEACH SLOPE : 1:69.56

SIGMA : 1.26 M.

TIME INTERVAL	RECESSION [M/YR]	$\frac{\lvert x_i - \bar{x} \rvert}{\sigma}$	AVG. EROSION [(M³/YR)/M]
1940 - 1956	-0.82	0.02	-6.89
1956 - 1966	-0.20	0.51	-1.68
1966 - 1980	-0.63	0.17	-5.29
1980 - 1984	-3.27	1.93	-20.44
1940 - 1984	-0.84	.....	-7.06
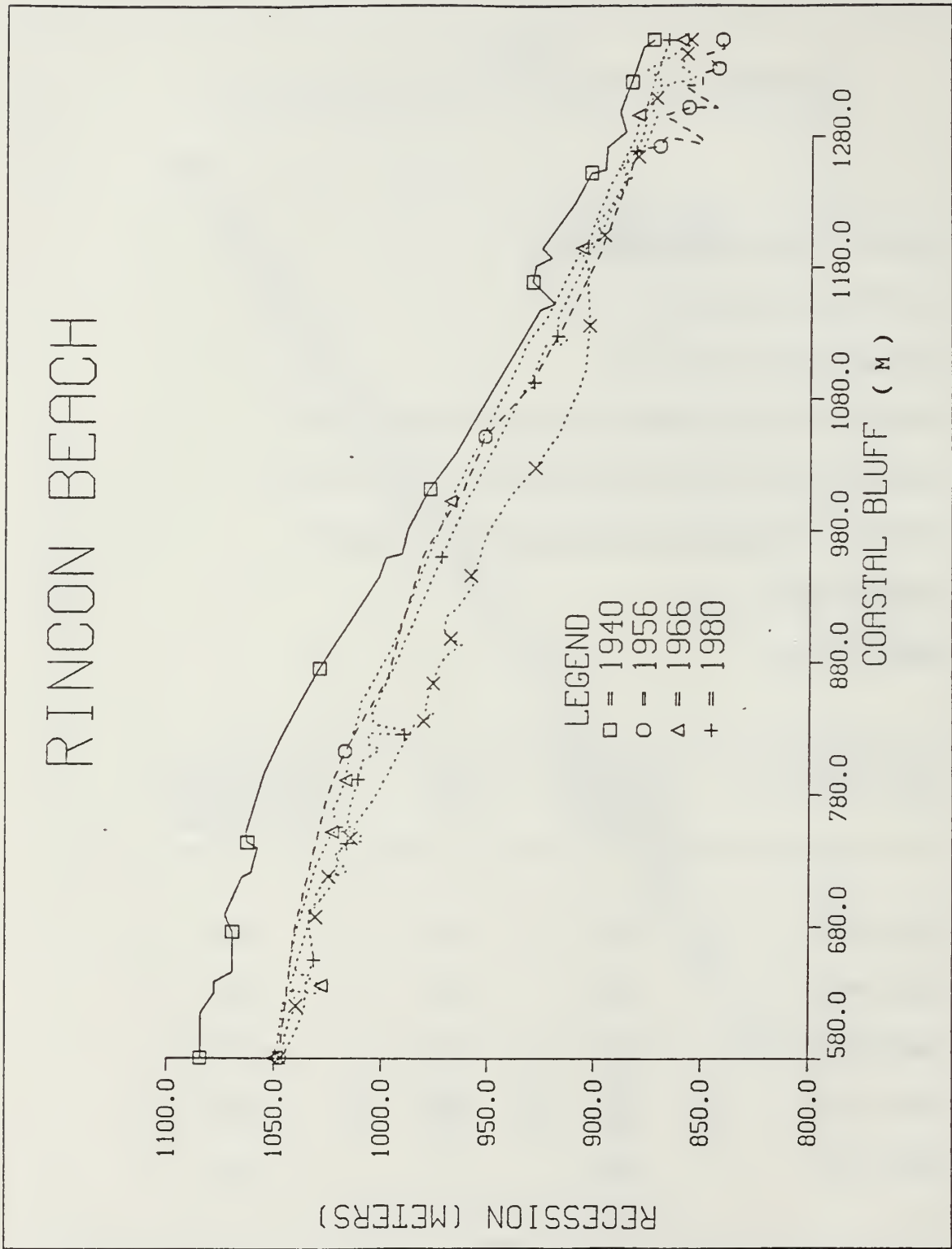
Figure 2.11   Rincon Beach Erosion Results.

TABLE VI
EROSION RATE RESULTS FOR MARINE LAB

STATION NAME : Marine Lab

LATITUDE : 36°47′35″ N

LONGITUDE : 121°47′32″ W

MEAN CLIFF TOE ELEVATION (above MLLW) : 5.15 M.

MEAN CLIFF TOP ELEVATION (above MLLW) : 8.93 M.

LONGSHORE OBSERVATION DISTANCE : 506.00 M.

BEACH SLOPE : 1:66.66

SIGMA : 1.63 M.

TIME INTERVAL	RECESSION [M/YR]	$\frac{|x_i - \bar{x}|}{\sigma}$	AVG. EROSION [(M^3/YR)/M]
1940 - 1966	+ 1.19	0.45	+ 10.63
1966 - 1970	-2.04	1.53	-18.22
1970 - 1976	+ 1.30	0.52	+ 11.61
1976 - 1984	-1.35	1.10	-12.05
1940 - 1984	+ 0.45	......	+ 4.02
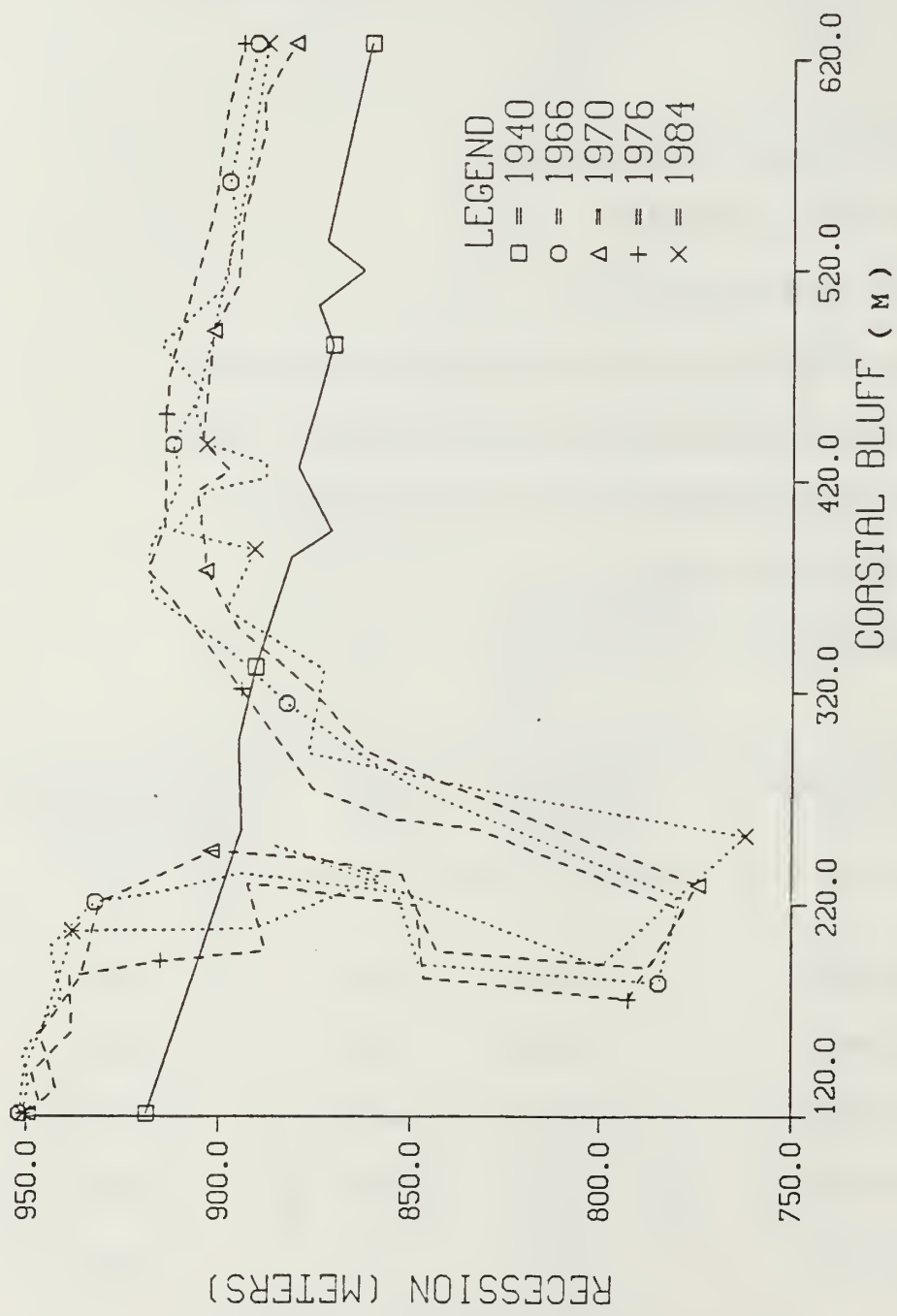
Figure 2.12   Marine Lab Erosion Results (Unsmoothed).
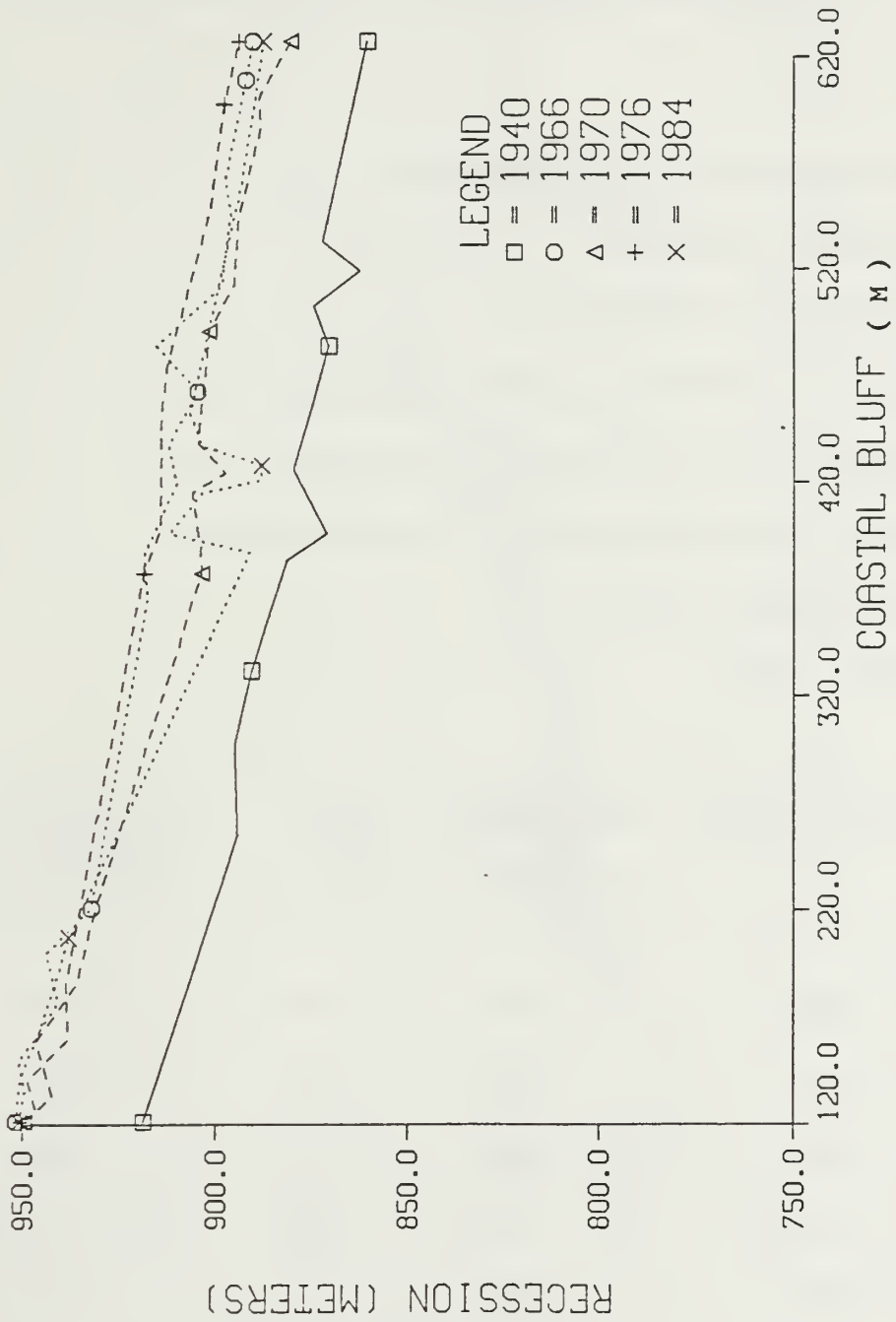
Figure 2.13   Marine Lab Erosion Results (smoothed).

43

TABLE VII
EROSION RATE RESULTS FOR NORTH MOSS LANDING

STATION NAME : North Moss Landing

LATITUDE : 36°48'25" N

LONGITUDE : 121°47'25" W

MEAN CLIFF TOE ELEVATION (above MLLW) : 5.29 M.

MEAN CLIFF TOP ELEVATION (above MLLW) : 9.81 M.

LONGSHORE OBSERVATION DISTANCE : 900.00 M.

BEACH SLOPE : 1:66.66

SIGMA : 2.08 M.

TIME INTERVAL	RECESSION [M/YR]	$\dfrac{|x_i-\bar{x}|}{\sigma}$	AVG. EROSION [(M^3/YR)/M]
1940 - 1970	+0.09	0.03	+0.88
1970 - 1976	+2.64	1.26	+25.99
1976 - 1980	-0.12	0.07	-1.47
1980 - 1984	-3.21	1.56	-31.78
1940 - 1984	+0.03	......	+0.29
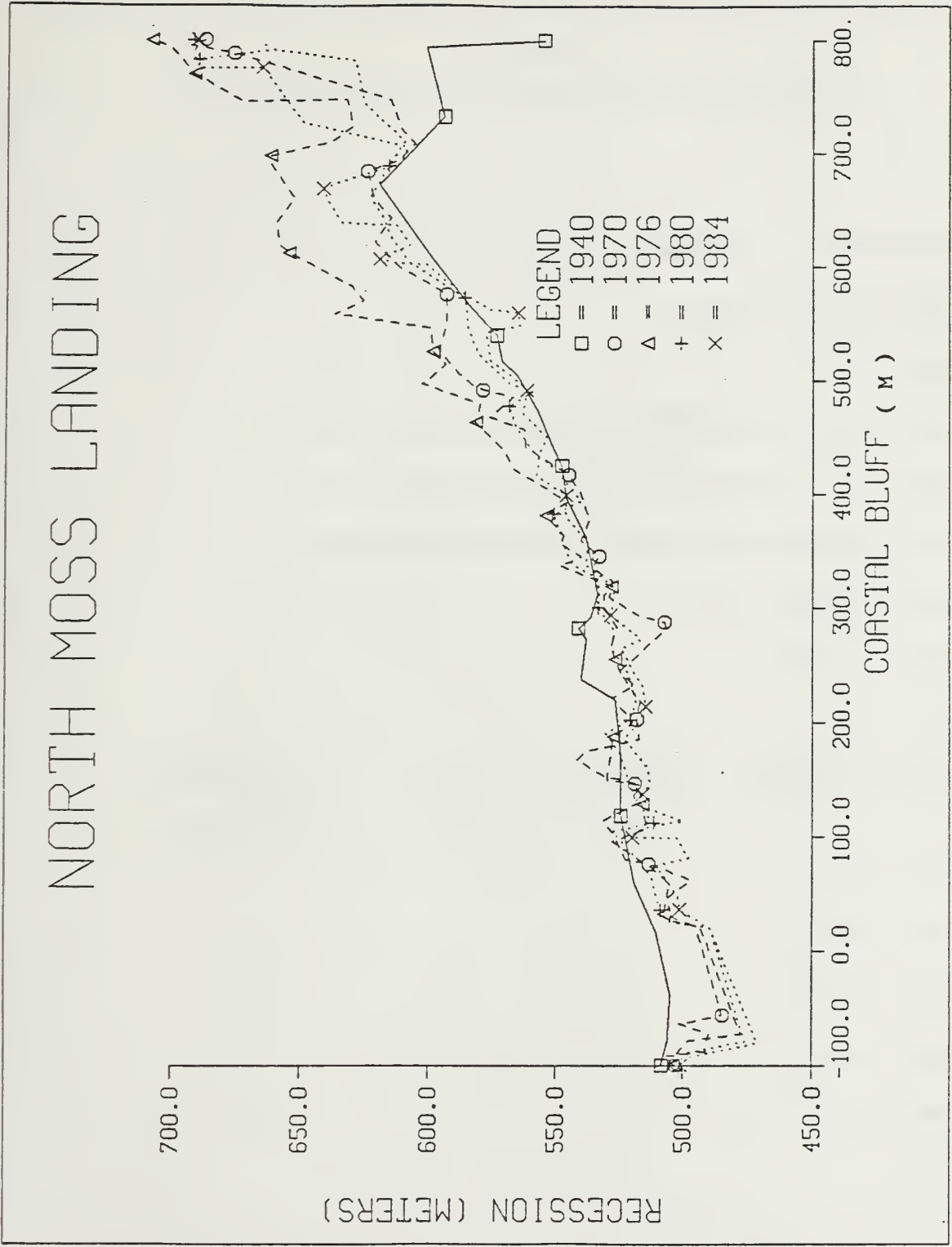
Figure 2.14   North Moss Landing Erosion Results.

TABLE VIII
EROSION RATE RESULTS FOR ZMUDOWSKI DUNES

STATION NAME : Zmudowski Dunes

LATITUDE : 36°49′40″ N

LONGITUDE : 121°47′50″ W

MEAN CLIFF TOE ELEVATION (above MLLW) : 3.26 M.

MEAN CLIFF TOP ELEVATION (above MLLW) : 15.56 M.

LONGSHORE OBSERVATION DISTANCE : 1050.00 M.

BEACH SLOPE : 1:69.55

SIGMA : 0.28 M.

TIME INTERVAL	RECESSION [M/YR]	$\frac{|x_i - \bar{x}|}{\sigma}$	AVG. EROSION [(M^3/YR)/M]
1940 - 1956	-0.16	1.28	-2.48
1956 - 1970	-0.84	1.14	-13.07
1970 - 1984	-0.61	0.32	-9.73
1940 - 1984	-0.52	......	-8.09
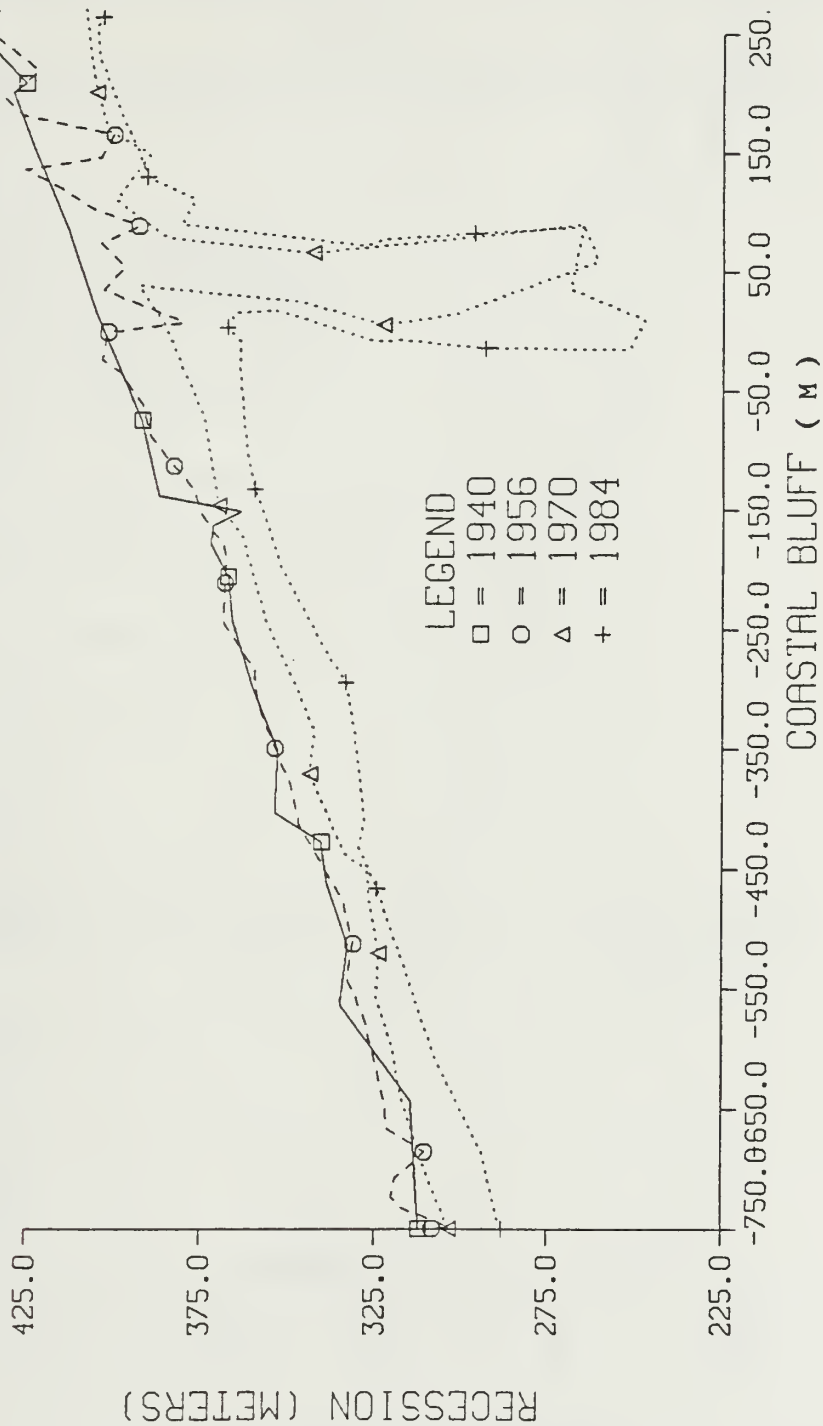
Figure 2.15   Zmudowski Dunes Erosion Results (Unsmoothed).

47
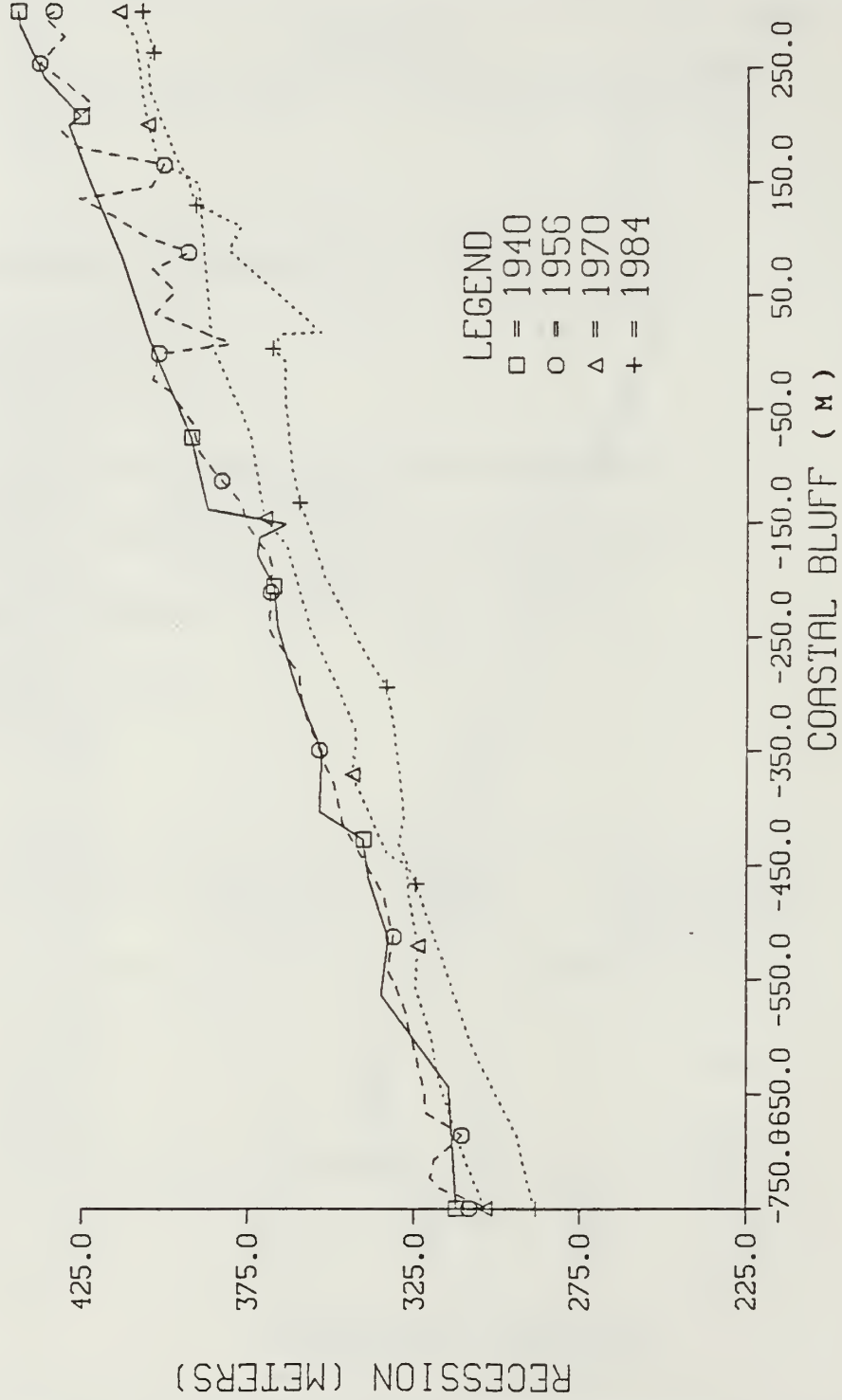
Figure 2.16   Zmudowski Dunes Erosion Results (Smoothed).

48

TABLE IX

EROSION RATE RESULTS FOR MONTEREY BAY ACADEMY

STATION NAME : Monterey Bay Academy

LATITUDE : 36°54′26″ N

LONGITUDE : 121°50′55″ W

MEAN CLIFF TOE ELEVATION (above MLLW) : 4.36 M.

MEAN CLIFF TOP ELEVATION (above MLLW) : 21.74 M.

LONGSHORE OBSERVATION DISTANCE : 1220.00 M.

BEACH SLOPE : 1:76.79

SIGMA : 0.64 M.

TIME INTERVAL	RECESSION [M/YR]	$\frac{\|x_i - \bar{x}\|}{\sigma}$	AVG. EROSION [(M³/YR)/M]
1940 - 1956	+0.18	0.79	+3.68
1956 - 1970	-1.33	1.45	-30.07
1970 - 1984	-0.03	0.04	-0.60
1940 - 1984	-0.33	......	-6.62
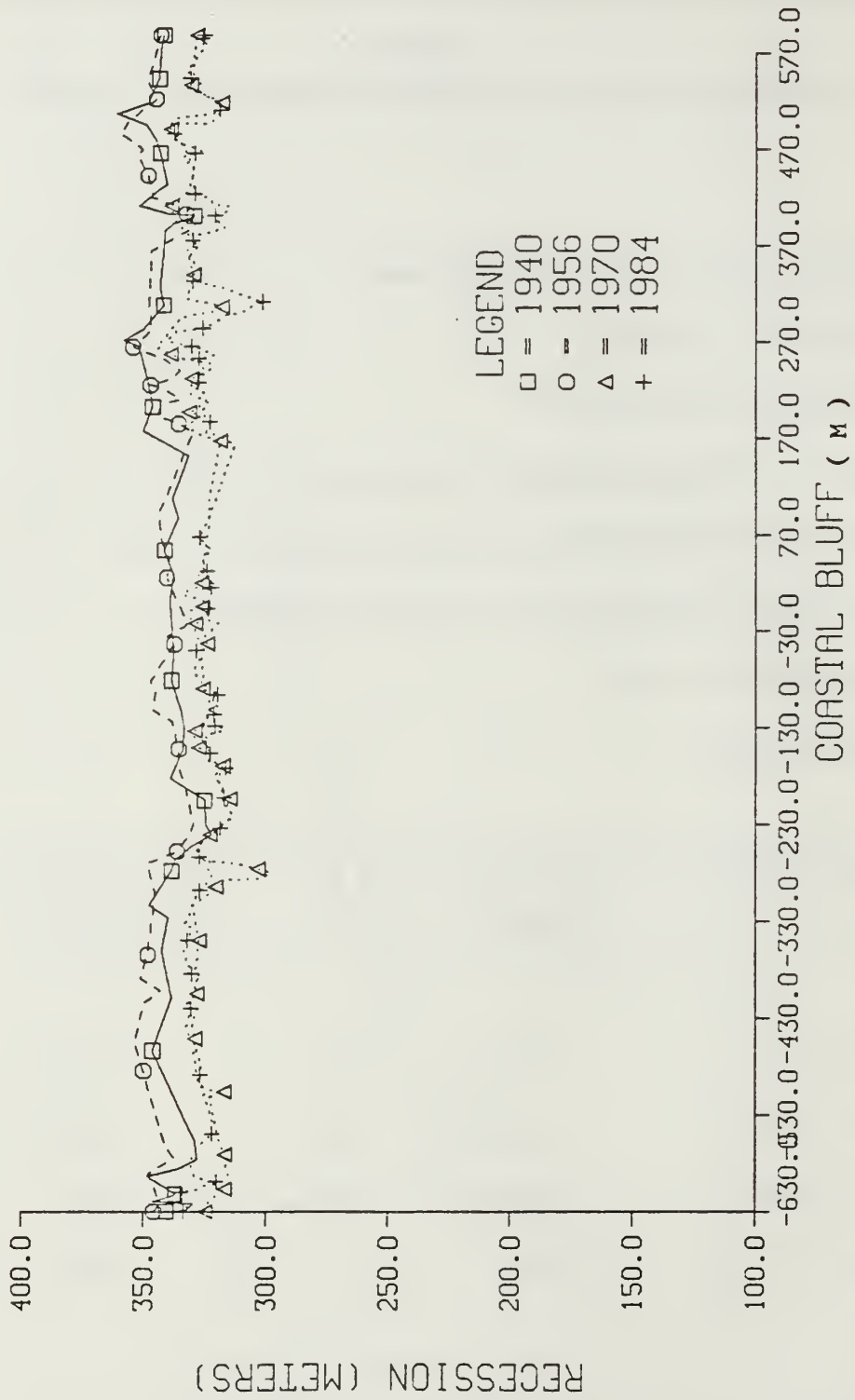
Figure 2.17   Monterey Bay Academy Erosion Results.

50

III. WAVES AND TIDES

A.   WAVE CLIMATOLOGY

An accurate understanding of wave climatology is paramount in any study of beach erosion. Wind waves provide the energy to drive the nearshore dynamics responsible for changes in coastal morphology. The wave climatology for Monterey Bay was calculated using the Wave Information Studies (WIS) deep water variance density spectra compiled by the U.S. Army Corps of Engineers. The WIS data is broken down into three phases. This study will be concerned with phases I and II only.

In phase I, wind fields are derived from the Gridded Northern Hemisphere Pressure Fields of the Navy Fleet Numerical Oceanography Center (FNOC), and the North American Historical Weather Map Series of the National Climatic Center (NCC). The data from FNOC and NCC represent a twenty year sampling from 1 January 1956 through 31 December 1975. A first guess wind field in regions of low streamline curvature is computed from quasi-geostrophic theory. Baroclinic effects caused by vertical temperature gradients (thermal wind) are added to the wind components and provide the basis for the observed ageostrophic flow. Wind fields for synoptic systems exhibiting strong streamline curvature, as typified by an extratropical cyclone, are derived from gradient wind theory which accounts for centrifugal acceleration in the balance of forces. Additionally, an isallobaric component of the wind field is estimated and included in rapidly developing systems where the rate of change in pressure with time cannot be ignored. The derived free atmospheric wind fields are then reduced to a boundary layer reference level using friction velocity scaling (Resio, Vincent, and Corson, 1982). Phase I wind information is computed with a six hour time step and interpolated to a 220 KM open ocean grid. In Phase II Surface Marine Observations and Airways Surface Observations, both available from NCC, are blended into the wind fields computed in phase I, and the modified wind fields are interpolated to a 55-km coastal grid.

Wind waves are hindcast using a discrete spectral wave model developed by Resio (1981). Two-dimensional variance density spectra are generated over sixteen

directional bands at 0.01-Hz frequency bands from 0.03 Hz to 0.22 Hz. Discrete spectral models, in general, are representative for waves in their late stages of development; however, they exhibit significant difficulty simulating proper growth in a fetch or duration limited domain, or for waves in their early stages of development (Dexter, 1974; Resio and Vincent, 1979). Barnet (1968) proposed a more complete specification of the classical A + BE(f) source term as a possible solution to this problem, where A represents the Phillips (1957) linear, initial wave growth mechanism, B, the Miles (1957) exponential, continued wave growth mechanism, and E(f) is the energy density spectrum. Although Barnet's term was three times too low for the JONSWAP spectrum, his initiative in incorporating a non-linear input aided in the subsequent parameterization of non-linear wave-wave interaction used in the Resio (1981) model. The non-linear source term employed by Resio (1981) is given by

$$G_{nl} = D \ \alpha^3 \ g^2 \ f_m^{-4} \ \exp[1 - (f_m/f)^4](f/f_m)^3 \tag{3.1}$$

From the JONSWAP data, $\alpha = 0.076X$, where X is the nondimensional fetch $X = gx/U^2$, D is a dimensionless constant, f_m is the frequency of maximum energy, and U is the wind velocity. The linear Phillips mechanism was found to transfer more energy into the low frequencies on the spectrum's leading edge than into the mid-range frequencies. It was consequently removed from the Resio (1981) model and replaced with the G_{nl} term in the source equation. The total source term for the Resio model is then given by the non-linear wave-wave interaction parameterization and the Miles exponential growth mechanism

$$S_{ource} = G_{nl} + B \ E(f) \ \psi(\theta - \theta_0) \tag{3.2}$$

In Equation 3.2, ψ is a nondimensional directional spreading function where θ_0 is the mean wind direction, and B is given by

$$B = s \ f[(u \ \cos\theta)c^{-1} - 0.9] \tag{3.3}$$

In Equation 3.3, s is the density ratio between the air and water, and c the phase speed, or celerity.

52

Clearly, with the Phillips mechanism missing, another wave generation scheme must be included to provide initial wave growth. This initialization is accomplished with a local parametric model. The domain of the parametric model is limited by a fixed high frequency cut off which delineates the boundary between the discrete spectral and parametric domains. The peak frequency is calculated for each time step from equations presented by Hasselmann et. al. (1976). The energy developed in the parametric domain is transferred to the discrete spectral domain until the peak frequency reaches the high frequency cut-off. The parametric spectrum then shifts to an f^{-5} equlibrium form, and all growth is continued in the discrete spectral domain. The Resio (1981) model provides wave growth and decay rates that are consistent with the observed JONSWAP data while maintaining spectral shapes that are highly representative of observed spectra (Risio, 1981). In phase I, wave information is calculated on a 220-km grid and the spectra are archived at 64 locations in the Pacific as depicted in Figure 3.1. In phase II, wave information is calculated using the modified wind fields at 55-km grid spacing and the spectra are archived at 53 coastal locations as depicted in Figure 3.2. Note that the wind wave model is a northern hemispheric model, and it does not allow wave energy from the southern hemisphere to propagate across the model's boundary.

B.   WAVE REFRACTION

Wave rays that approach non-parallel isobaths at an oblique angle will tend to bend toward the orthogonals of the isobaths as a result of wave refraction. Consequently, an area where rays come together is a region of energy convergence, and an area where rays separate, a region of energy divergence. In Monterey Bay the Moss Landing area at the head of Monterey Canyon provides a good example of energy divergence; conversely, Fort Ord typifies a region of ray focusing, or energy convergence.

The effects of shoaling (changing group velocities) and refraction (convergence or divergence of variance density) are applied to the WIS deep water spectra to provide shallow water and surf zone information. The variance density transformation is performed using spectral ray theory. In spectral ray theory, one assumes that energy, or variance, that is associated with a particular frequency and directional band will remain in that band throughout the transformation, i.e. constant energy flux (Thornton, 1983). Hence the shallow water variance density spectra $S_h(f,\theta)$ are related to the deep water variance density spectra $S_0(f_0,\theta_0)$ by
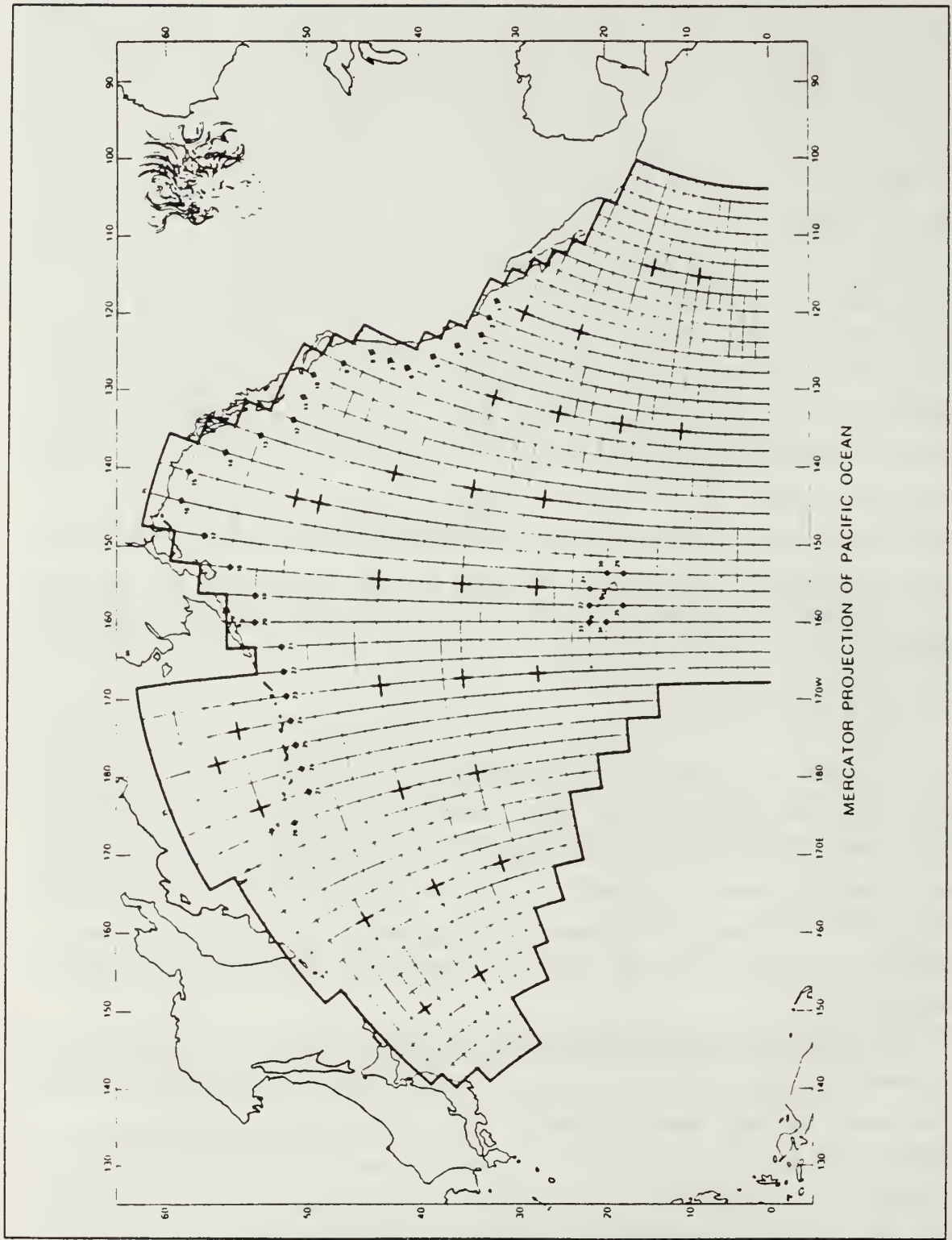
Figure 3.1 WIS Phase I Grid
with Archive Locations Indicated.

54

$$S_h(f,\theta) = K^2_r(f,\theta) \, K^2_s(f) \, S_0(f_0,\theta_0) \, J \tag{3.4}$$

where Kr is the refraction coefficient, Ks the shoaling coefficient, and J is the Jacobian of the transform.

Here, $J = \partial(f_0,\theta_0)/\partial(f,\theta)$

however, since $f_0 = f$, J becomes $\partial(\theta_0)/\partial(\theta)$ and integrates away.

The shoaling coefficient, Ks, is given from Airy wave theory to first order as the ratio of the deep and shallow water group velocities.

$$Ks = \sqrt{(C_{g0}/C_g)} \tag{3.5}$$

where C_g is given by

$$C_g = C/2(1 + 2kh/\sinh 2kh) \tag{3.6}$$

In shallow water, surface gravity waves become non-dispersive and the group velocity can be approximated by

$$C_g = C = \sqrt{(gh)} \tag{3.7}$$

The deep water group velocity is fixed for a particular frequency, whereas the shallow water group velocity will change with shoaling water depths; hence Ks will increase as the wave crest approaches the shore.

The refraction coefficient, Kr, provides a measure of ray separation

$$Kr = \sqrt{(b_0/b)} \tag{3.8}$$

where b_0 is the deep water ray separation, and b is the shallow water ray separation. Values of Kr that are greater than unity represent energy convergence, and those less than unity, represent energy divergence. The refraction coefficients for this study were calculated using the linear refraction model by Dobson (1967) modified to refract rays from a specified shallow water location, back to deep water. This "back" refraction

Figure 3.2   WIS Phase II Grid
with Archive Locations Indicated.

model was developed to obtain refractive information at specific locations. The model searches for the 4-m isobath along a normal to the shoreline that originates at an observation site or other point of interest. Rays for each frequency in the WIS spectrum (0.03 Hz - 0.18Hz) are started at a specified location and depth, nominally 4-m, and are propagated offshore at 0.1-degree increments over the range of all possible arrival angles. Once in deep water, the rays are sto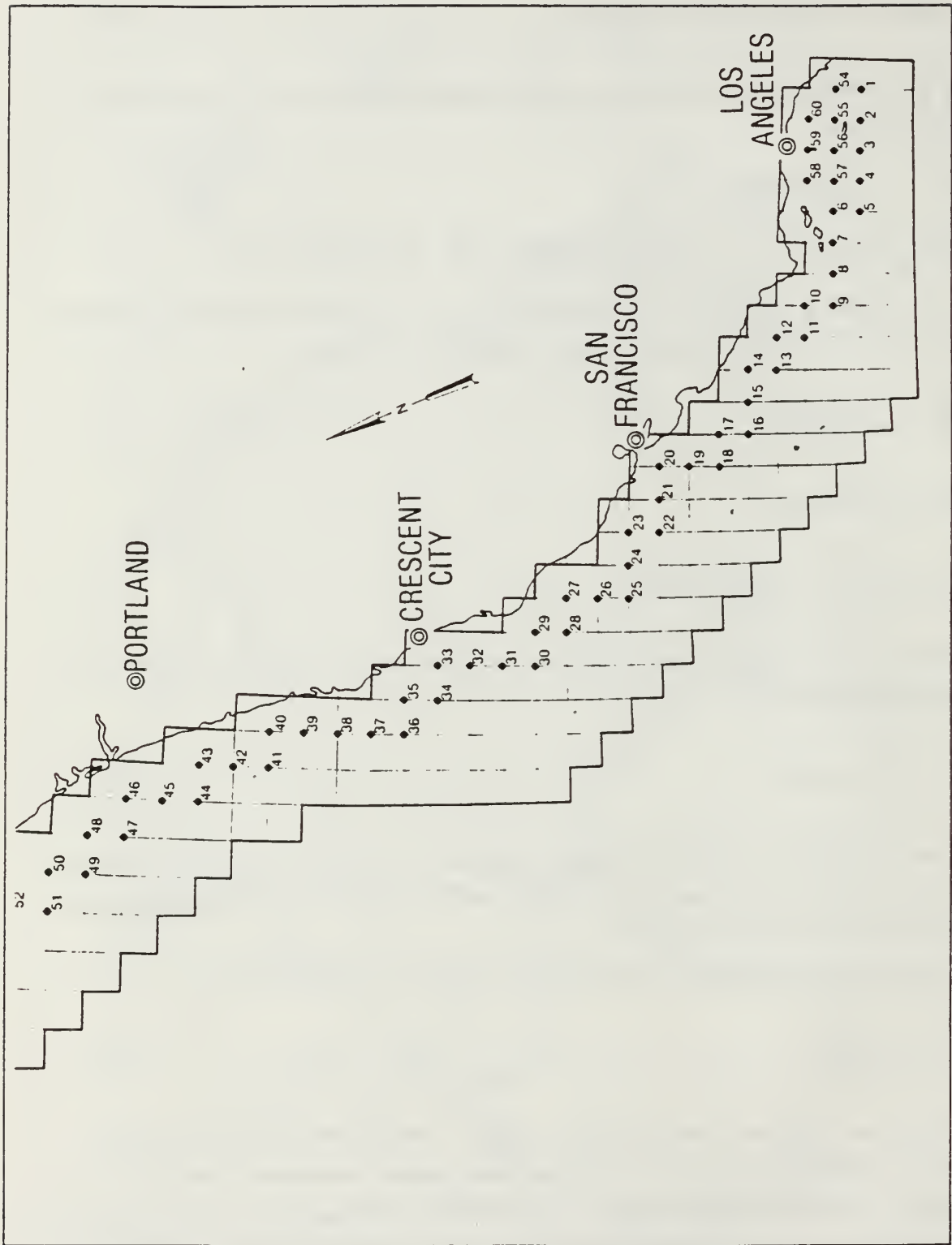pped and the deep water angle is measured; then they are turned around and propagated back inshore along the same path to calculate the spectral refraction coefficient. The rays must return to the initial location within the specified area of ± 100 m to be a valid calculation. Examples of spectral refraction in Monterey Bay are presented in Figures 3.3, and 3.4.

The bathymetry used in the refraction model is critical to the analysis. The accuracy of the calculated refraction information can be no better than the accuracy of the bathymetry; consequently, considerable effort was devoted to accurately depict the bottom. Original NOAA data was obtained that had been projected onto a six-second modified Universal Transverse Mercator (UTM) grid. The bathymetry data was initially screened for bad points, then the data was scanned along meridians and parallels for changes in slope that exceeded $30°$. Points that generated unrealistic bathymetry were extracted from the data base, and the resultant bathymetry was projected onto an x-y plane via a modified UTM projection. The bathmetry was interpolated to a 200-m rectangular grid using a piecewise-linear, triangular plane interpolator (Franke, 1986). The triangulation method provided reasonable results in data sparce regions, and minimum distortion of bathymetric features. Intermediate smoothing was accomplished using a nine point weighted linear averager, and further smoothing was provided by the model itself which calculates bottom curvature by fitting a quadratic surface to adjacent isobaths. Waves originating from the northerly most quadrant are refracted when travelling over the shoal shelf region between the Farallon Islands, and Point Santa Cruz. To include the refraction to the north, a supplemental Northern bathymetry was gridded for a section of the California coast north of Santa Cruz. Refraction coefficients were calculated for the portion of the ray path which traversed the northern bathymetry, and for the portion of the ray path in Monterey Bay. The two refraction coefficients were multiplied together to determine a complete refraction coefficient for use in the spectral transformation. The Monterey Bay bathymetry is shown in Figure 3.5.

57
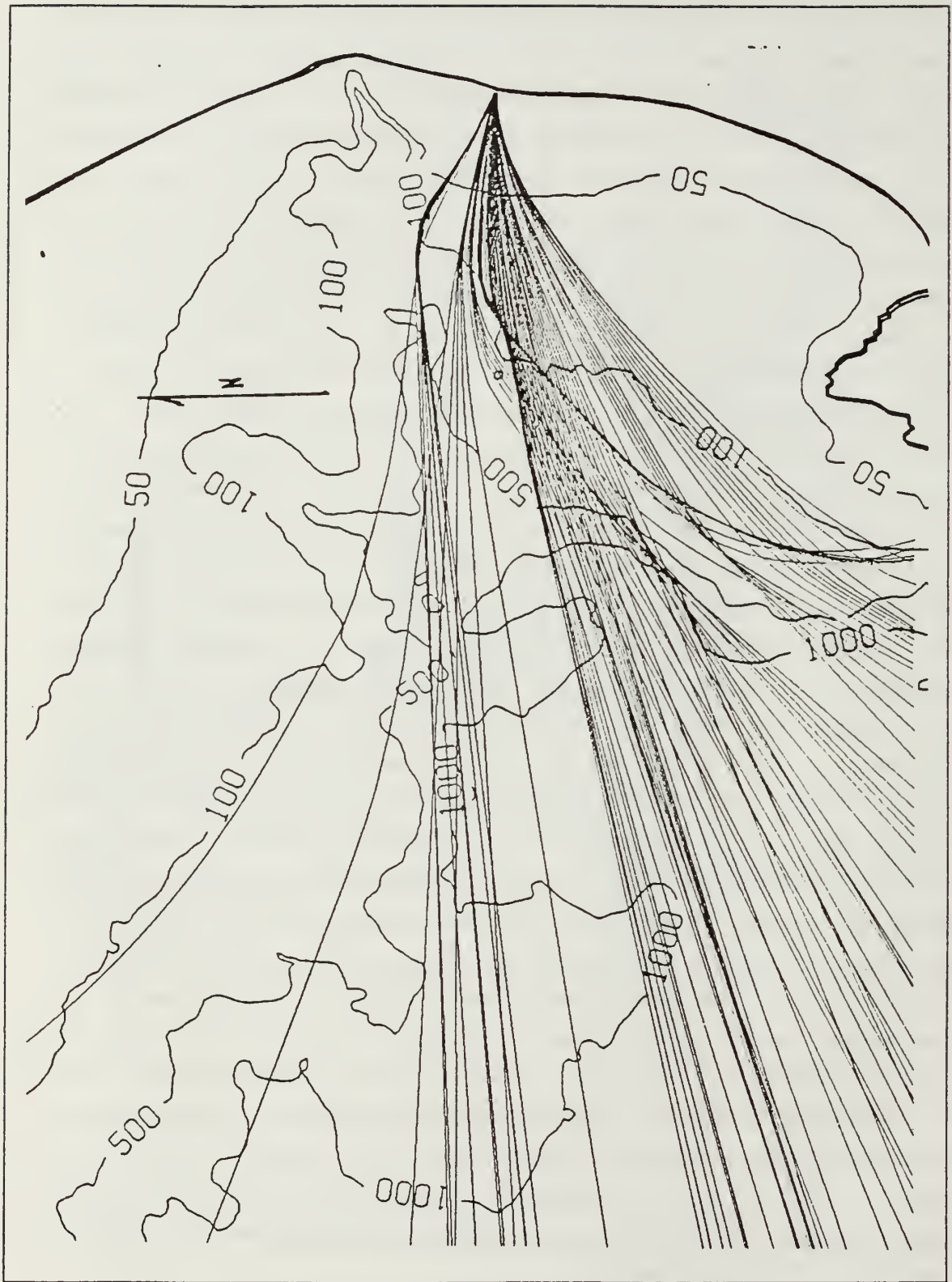
Figure 3.3   Ray Trace for Marina, f = 0.05 Hz..

58

The objective in performing the spectral transformation is to produce a wave height that can be used to calculate wave set-up, run-up, and energy. The significant wave height, Hs, is related to the total energy, or variance, σ^2, by

$$H_s = \sqrt{2}(H_{rms}) \sim \sqrt{2}\sqrt{(8\,\sigma^2)} \sim 4\sigma \qquad (3.9)$$

The variance is calculated by integrating the transformed shallow water spectrum over all frequencies and directions.

$$\sigma^2 = \int_f \int_\theta S_h(f,\theta)\, df\, d\theta \qquad (3.10)$$

C.   WAVE SET-UP AND RUN-UP

As waves break in the surf zone, they transfer momentum shoreward. The change in shoreward momentum flux is primarily balanced by hydrostatic pressure; accordingly, the hydrostatic pressure balance is maintained through an increase in the mean sea level shoreward of the surf zone. This balance assumes that there are no mean currents, and no longshore gradients in the shoreward momentum flux, and is given by

$$\partial/\partial x[2EC_g/C - E/C] = -\rho g(\eta + h)\partial\eta /\partial x \qquad (3.11)$$

where the term in brackets on the left hand side is the momentum flux due to the normally incident breaking waves. As waves break, the wave energy, E, decreases resulting in a decrease in momentum flux, i.e. negative gradient, which must be balanced by a positively sloping sea surface. This mechanism is known as set-up (η) and its maximum height above mean sea level occurs at its shoreward limit. Wave set-up studies by Guza and Thornton (1981) suggest that wave set-up is proportional to the deep water RMS wave height. Additional work by Holman and Sallenger (1985) over a wider range of wave and beach parameters, corroborate the results of Guza and Thornton, and further suggest that there is a correlation between the tidal stage, and wave set-up. Beach erosion primarily occurs at high tide, and consequently this study uses wave set-up at high tide (Holman and Sallenger, 1985).

59
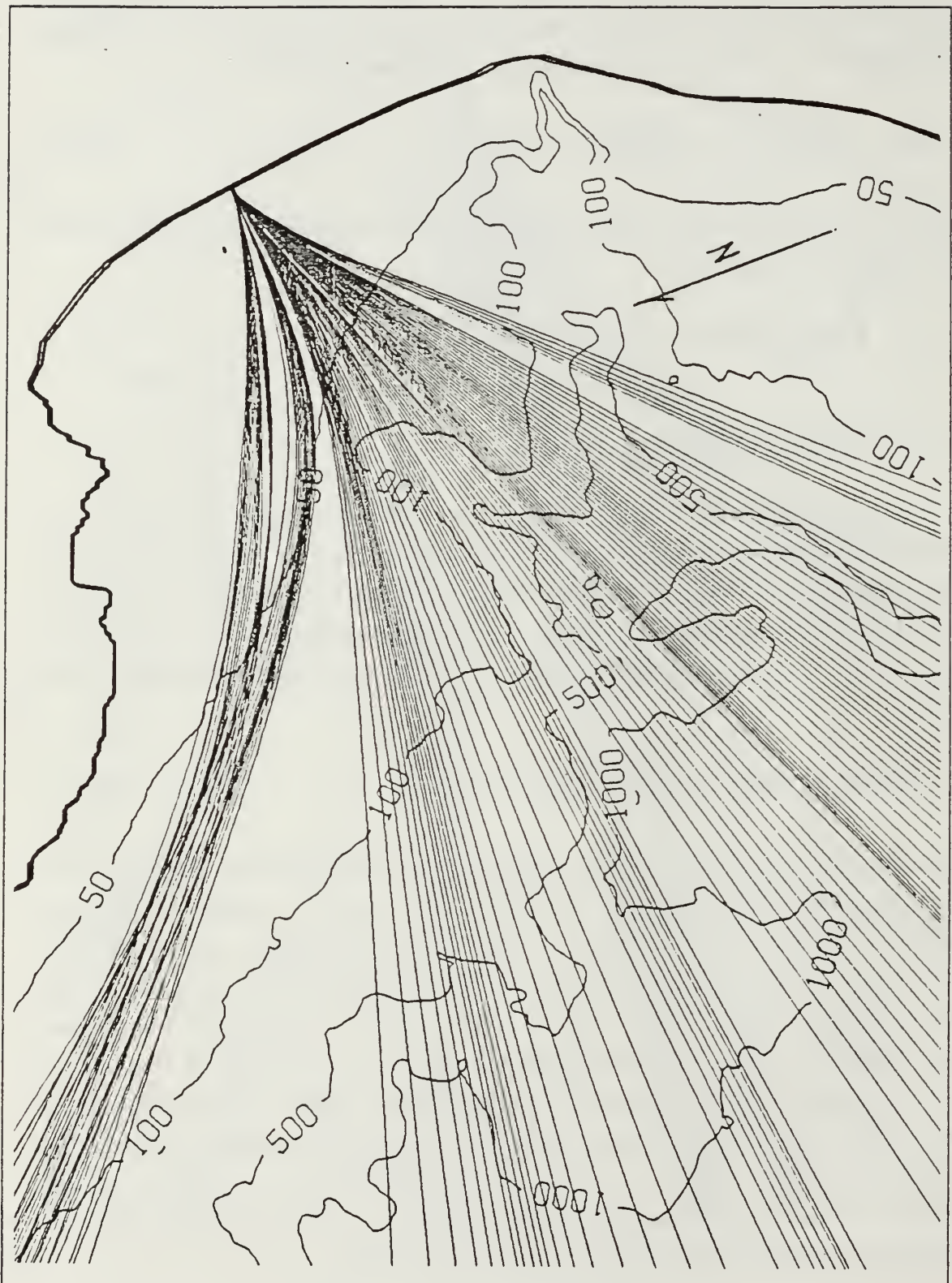
Figure 3.4   Ray Trace for M.B. Academy, f = 0.09 Hz..

60

$$\eta = 0.88 H'_{s0} \qquad (3.12)$$

The significant wave height, H_s is calculated at the 4-m isobath, where $H_s \sim 4\sigma$, then the wave is back shoaled without refraction to obtain a deep water significant wave height, H'_{s0}, using

$$H'_{s0} = Hs/Ks \qquad (3.13)$$

where Ks is calculated using the peak frequency. Wave set-up is dipicted in Figure 3.7.

Wave run-up is the maximum superelevation of the sea level caused by the rush of breaking waves up the beach. Thornton and Guza (1981) suggest that run-up is also proportional to the deep water wave height H'_{s0}. Holman and Sallenger (1985) note a tidal correlation and find run-up at high tide to be given by

$$\eta = 0.14 H'_{s0} \qquad (3.14)$$

Wave set-up and run-up are important parameters in raising the mean sea level to a stage where waves can erode the cliff base.

D.   TIDES

The calculation of tidal height is inherently critical to the specification of mean sea level. The simultaneous presence of high tide and storm waves presents the highest probability that an erosion event will occur. Consequently, any parameterization of the fluxuating sea surface must include a harmonic tidal analysis. The harmonic analysis allows one to express the tidal height at any time, t, as a finite sum of its harmonic constituents, each of which is representative of a specific astronomic condition. The tidal expression from Dennis and Long (1971) is presented below

$$h = H_0 + \sum\nolimits^n f_n H_n \cos[a_n t - (k_n - [V_0 + u]_n)] \qquad (3.15)$$

where H_0 is the height of the mean tidal level (above datum), f_n is the node factor of the constituent, H_n is the mean amplitude of the constituent, a_n is the speed of the constituent, t is the time reckoned from some arbitrary point, k_n is the epoch of the constituent at t = 0 for the observation period, $[V_0 + u]_n$ is the value for the
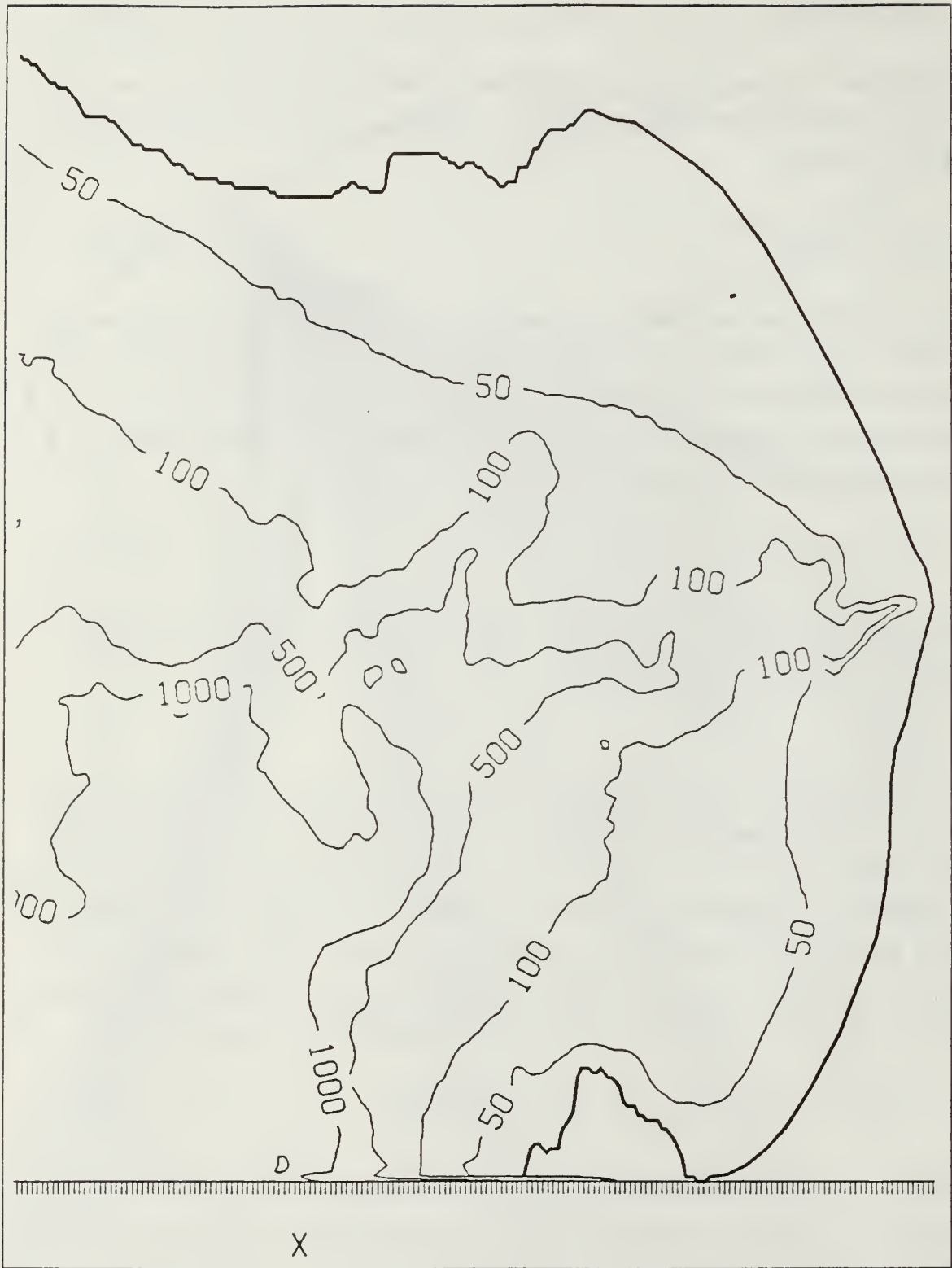
Figure 3.6 Bathymetry of Monterey Bay.

argument at t = 0 for the observation period, and n is the particular constituent being computed.

The constituents for Monterey Bay were obtained from a harmonic tidal analysis performed by the Tidal Predictions Branch of the National Ocean Service. Their data base was a thirteen-year time series of tidal data observed at Monterey's Municipal Wharf No. 2. Twenty constituents were isolated with the threshold criterion that a constituent would be consideried valid only if its amplitude contribution was greater than 0.6 cm. The speed, node factor, and argument of the constituents were extracted from Schureman (1971). The twenty constituents were used to calculate tidal heights at every hour during the twenty-year WIS time series.

The tides in Monterey Bay are typically semi-diurnal with two low and two high water cycles per day. The mean tidal range is 0.98 m.
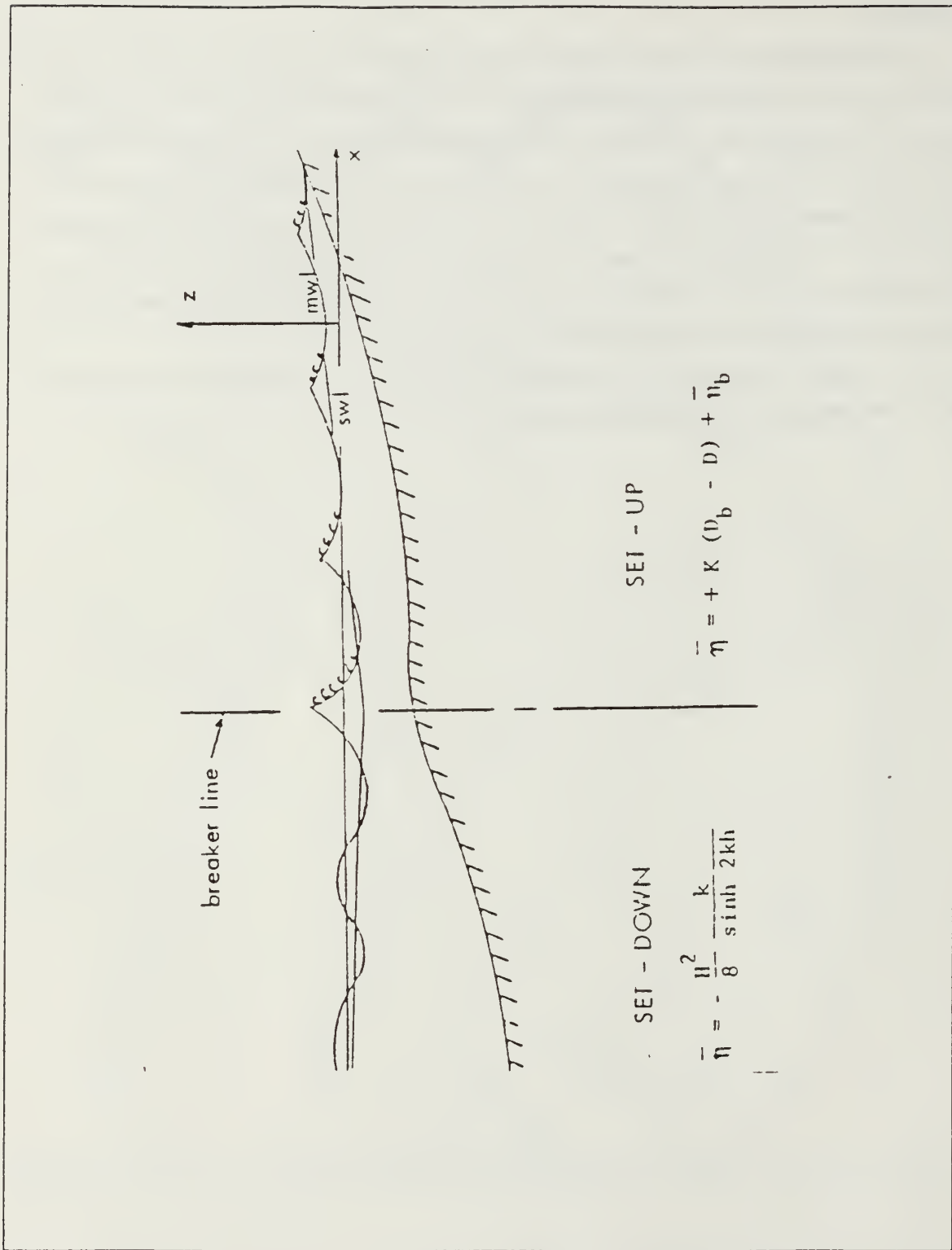
Figure 3.7   Wave Set-up.

IV. AN EROSION MODEL FOR MONTEREY BAY

A.   MODEL PRESENTATION

The objective of this thesis is to develop an erosion model for Monterey Bay. Lima and Sklavidis (1984) computed a multiplicative constant, k, for the Brunn erosion model presented in Komar (1983)

$$R = k[(S - T)/\tan\beta]$$ (4.1)

where R is the recession rate, S is the height of mean sea level, T is the cliff toe elevation, $\tan\beta$ is the beach slope. The value k = 0.000098 was calculated from a linear regression of the Lima and Sklavidis (1984) recession rate data to the Brunn model.

This research presents a model where recession is a non-linear function of the deep water significant wave height H'_{s0} (for purposes of clarity in the following equations, H'_{s0} will be replaced by H).

$$R_{mod} = [AH^2 + BH + C(S - T)]/\tan\beta$$ (4.2)

R_{mod} is the modeled recession rate and A, B, and C are constants. The deep water significant wave height is determined as discussed in Chapter III and the mean sea level, S, is given by

$$S = Tide + Set\text{-}up + Run\text{-}up$$ (4.3)

The beach slope, $\tan\beta$, was extracted from large scale hydrographic charts and varied little along the Bay. The idea of the model is that bluff recession only occurs when superelevation of the mean sea level, caused by tides and waves, exceeds the height of the cliff toe. When this criterion has been met, recession will occur at a rate which is proportional to: the wave energy, AH^2, the significant wave height, BH, and the ammount of water which exceeds the cliff toe, C(S-T).

In solving for A, B, and C, it is necessary to minimize

$$\sum (R_{mod} - R_{obs})^2 = MIN \qquad (4.4)$$

where R_{obs} are the recession rates observed during the time-span of the WIS spectral data from 1956 to 1975. The partial derivatives of equation 4.4 are taken with respect to A, B, and C, and set equal to 0 to define the following three normal equations

$$A\sum H^4 + B\sum H^3 + C\sum (S\text{-}T)H^2 = Tan\beta \sum R_{obs}H^2 \qquad (4.5)$$

$$A\sum H^3 + B\sum H^2 + C\sum (S\text{-}T)H = Tan\beta \sum R_{obs}H \qquad (4.6)$$

$$A\sum H^2(S\text{-}T) + B\sum H(S\text{-}T) + C\sum (S\text{-}T)^2 = Tan\beta \sum R_{obs}(S\text{-}T) \qquad (4.7)$$

The three equations are then solved simultaneously by the matrix equation

$$\begin{bmatrix} \sum H^4 & \sum H^3 & \sum (S\text{-}T)H^2 \\ \sum H^3 & \sum H^2 & \sum (S\text{-}T)H \\ \sum H^2(S\text{-}T) & \sum H(S\text{-}T) & \sum (S\text{-}T)^2 \end{bmatrix} \times \begin{bmatrix} A \\ B \\ C \end{bmatrix} = \begin{bmatrix} Tan\beta \sum R_{obs}H^2 \\ Tan\beta \sum R_{obs}H \\ Tan\beta \sum R_{obs}(S\text{-}T) \end{bmatrix} \qquad (4.8)$$

This procedure is repeated for each of the twelve stations and the resultant coefficients are averaged to determine a mean A, B, and C for Monterey Bay.

The model is very sensitive to changes in the elevation of the cliff toe, as this elevation is the model's go, no-go threshold value. An initial mean sea level model was run at each station to determine the number of hours, N, that the sea height exceeded the cliff toe for the twenty year WIS data. Adjustments , less than 0.5 m, were then made to the surveyed cliff toe elevation to ensure that the modeled N for each station was physically reasonable, and its value was within one order of magnitude of the other stations. The adjustments themselves are not unreasonable considering the inherent

66

variability of the cliff toe elevetion due to falling cliff material, and seasonal sediment transport.

B. DISCUSSION OF RESULTS

Recession model coefficients A, B, and C are determined for all sites that exhibit recession between 1956 and 1975. Moss Landing Marine Laboratory, and North Moss Landing are the only sites where continuous accretion during the time period prevented application of the model. Initial variance and standard deviation values are determined for the coefficients at the remaining ten sites, and based on this initial analysis, the coefficients for Monterey Sand Co. are rejected as being statistically unrepresentative of the erosion processes in Monterey Bay. The coefficients of the remaining nine sites are averaged to provide a mean A, B, and C, and hence define the recession model. These coefficients are listed in Table X.

The calculated mean values of the coefficients provide a reasonable depiction of bluff recession for regions of low wave energy, and will heretofore be referred to as the Low Energy Model. The linear wave height coefficent B, is the most significant, and defines a mildly sloping recession profile. Unfortunately, as can be seen in Figure 4.1, the Low Energy Model becomes unreliable in regions of energy convergence. A significant wave height of 5 m appears to be the threshold where the model's energy term, AH^2 , begins to have a significant impact on the model recession. Hence a new value, A_{HE} , for the energy coefficient, A must be determined from a weighted average of the A coefficients computed in the following regions of high wave energy: South Fort Ord, Stillwell Hall, Marina, and Monterey Bay Academy (see Table X). A High Energy Model is then obtained by replacing A with A_{HE} . The coefficients B and C remain the same as in the Low Energy presentation, however, the new, A_{HE} parameterization of the modelled energy produces a much more realistic model response in energetic regions. This improved response is also depicted in Figure 4.1. The high energy recession curve is too shallow at low wave heights and consequently, the model overpredicts the observed recession in these regions.

TABLE X
CALCULATED RECESSION COEFFICIENTS

Station Name	A $[1/M^2]$	B $[1/M]$	C $[1/M]$
NPS Beach Lab	-0.058619	0.233661	-1.79972×10^{-2}
Phillips Petroleum	-0.025892	0.144141	-2.29962×10^{-3}
Sand City	-0.052943	0.358974	-2.59265×10^{-3}
Monterey Sand Co.	-0.063531	0.461977	-1.83579×10^{-2}
South Fort Ord *	-0.011144	0.133575	5.18795×10^{-4}
Stillwell Hall *	-0.023181	0.233329	2.43953×10^{-3}
Marina *	-0.016920	0.196066	-1.20543×10^{-3}
Rincon Beach	-0.010737	0.101922	5.60665×10^{-5}
Zmudowski Dunes	-0.020776	0.188279	-2.08930×10^{-3}
Monterey Academy *	-0.023647	0.228347	3.02067×10^{-3}
Mean Values	-0.027095	0.20203	-0.002317
High Energy values *	-0.020051	same	same
Standard Deviations	± 0.0287	± 0.2143	± 0.0024

* Indicates regions of high wave energy, $H'_{s0} \geq 5$ m.
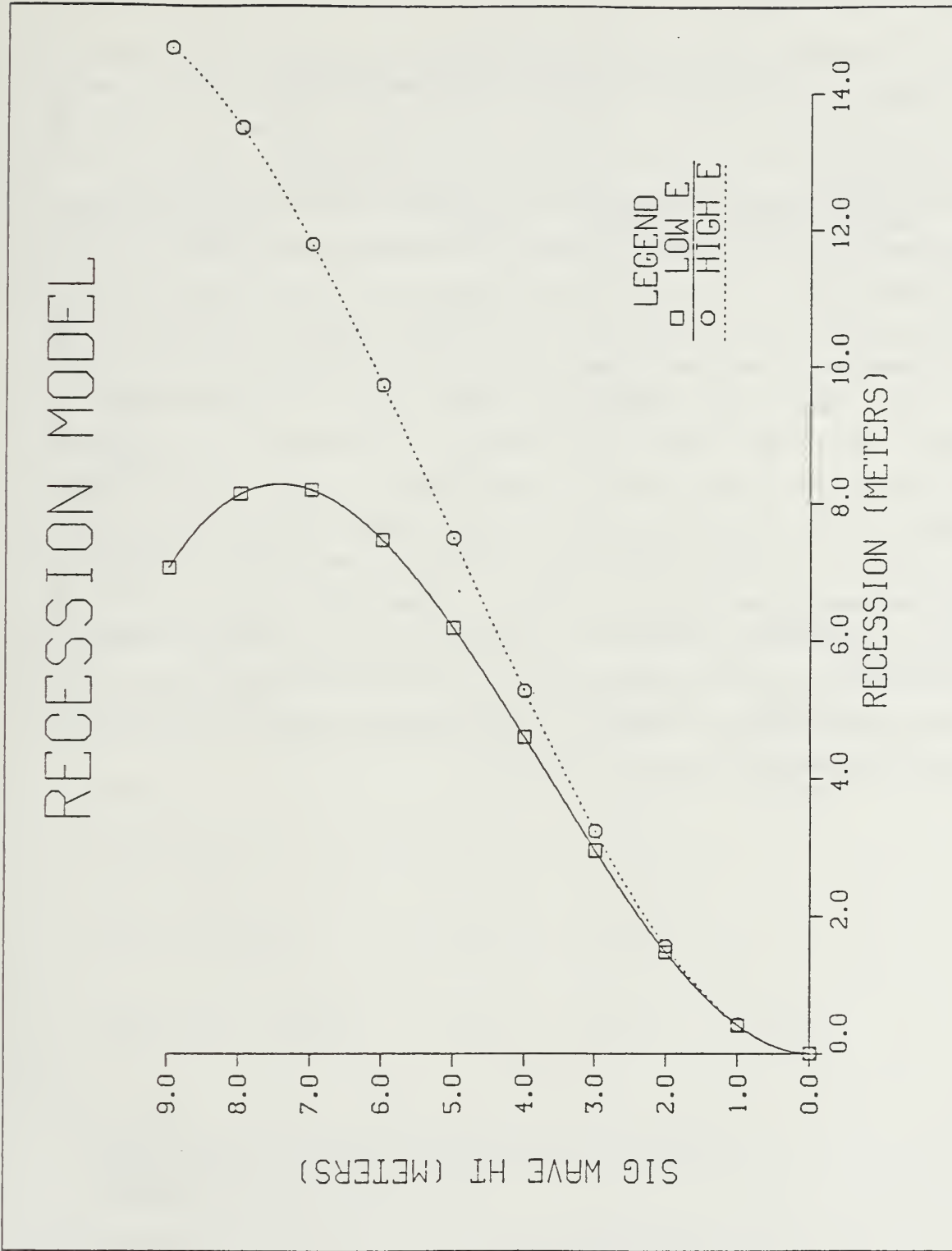
Figure 4.1   Recession Model Profile.

69

C. CONCLUSIONS

The recession rates are found to be related to the local wave height. A polynomial regression model in wave height shows the recession to be most correlated with wave height to the first power (B is the largest coefficient) and negatively correlated with wave energy, H^2. The recession observations at Sand City and Monterey Sand Company show significantly more bluff recession than the Low Energy Model suggests, and the observed significant wave height does not warrent use of the High Energy Model. Local sand mining operations are the most probable cause for the high recession values at these sites. For the remaining eight stations, however, the most representative results are obtained by applying the Low Energy Model in regions of low wave energy, and the High Energy Model in regions of high wave energy. In doing so, the standard error calculated between the observed and the computed twenty-year recession rates is ± 3.41 m which equates to ± 0.17 m/yr. The mean recession rate for the stations which experienced recession between 1956 and 1975, discounting stations Sand City and Monterey Sand Company, is 0.76 m/yr, hence the model represents actual recession to ± 22 %. These results are listed in Table XI. Graphic depictions of the twenty year recession at each site are depicted in Appendix C. The observed recession results presented in Table XI only represent events occuring between January 1956 and December 1975, and a complete summary of bluff recession between 1940 and 1984 is provided in Table XII.

TABLE XI
RECESSION MODEL RESULTS (1956-1975)

Station Name	Observed	Modelled	High Energy Model
NPS Beach Lab	9.00 m	11.45 m	
Phillips Petroleum	7.80 m	13.43 m	
Sand City	23.80 m	14.4 m	
Monterey Sand Co.	33.0 m	14.86 m	
South Fort Ord	15.8 m	10.57 m	19.68 m
Stillwell Hall	19.40 m	10.97 m	20.49 m
Marina	22.4 m	12.36 m	23.49 m
Rincon Beach	9.60 m	13.56 m	
Zmudowski Dunes	16.80 m	14.08 m	
Monterey Bay Academy	21.8 m	13.51 m	19.97 m

The Standard Deviation for the Model is $\pm$ 3.41 m for 20 years which equates to $\pm$ 0.17 m/yr.

TABLE XII
OBSERVED RECESSION SUMMARY

Station Name	Recession (m/yr)
NPS Beach Lab	-0.58
Phillips Petroleum	-0.85
Sand City	-0.97
Monterey Sand Co.	-1.94
South Fort Ord	-1.12
Stillwell Hall	-1.98
Marina	-0.38
Rincon Beach	-0.84
Marine Lab	+0.45
North Moss Landing	+0.03
Zmudowski Dunes	-0.52
Monterey Bay Academy	-0.33
Standard Deviation	±0.73 Mean = -0.75 m/yr

APPENDIX A

PROGRAM LISTING PHOTODAT

```
2 INPUT "WHAT IS YOUR STATION I.D. I.E. LAB1956":E$
3 OPEN E$ FOR OUTPUT AS #1
4 PRINT
5 PRINT FILE$
7 PRINT
8 COUNT=0
9 PRINT "REMEMBER TO ALWAYS APPROACH YOUR POINT FROM THE SAME DIRECTION"
10 PRINT "TO PREVENT ELECTRONIC OR MECHANICAL BACKLASH FROM OCCURING IN"
11 PRINT "THE DATA.  THE FIRST STEP IS TO DEFINE YOUR ORIGIN.  MOVE THE"
12 PRINT "VIEWER OVER THE CORRECT POINT AND PRESS ( DH ) (RETURN) AT THE"
13 PRINT "( : ) PROMPT.  REPEAT THIS PROCEDURE FOR EACH AXIS."
14 PRINT
15 GOTO 20
16 PRINT
18 PRINT
19 PRINT "REDEFINE THE ORIGIN, PRESS ( DH ) AT THE PROMPT"
20 FOR I=1 TO 3 STEP 2              ' THIS LOOP INITIALIZES THE X&Y AXES
25 J=I-1                            ' N= THE DMC-400 READ/WRITE ADDRESS
30 N=1000+J                         ' N=1000 X-AXIS N=1002 Y-AXIS
35 A=1                              ' AXIS COUNTER. X=1 Y=2
40 PRINT CHR$(INP(N)):
45 B=INP(N+1)                       ' CHECKS DMC-400 STATUS ADDRESS
50 C=INT(B/2)                       ' "C" CHECKS STATUS FLAG BIT
55 IF C=B/2 THEN 80                 ' DOES DMC-400 HAVE DATA TO SEND?
60 IF INT(C/2)=C/2 THEN 45          ' IS DMC-400 READY TO ACCEPT COMMANDS?
65 IF A=4 THEN 95
70 A$=INKEY$                        ' INPUT COMMAND FROM KEYBOARD
71 IF LEN(A$)=0 THEN 45
72 PRINT A$:
75 OUT N, ASC(A$)                   ' SEND THE "DEFINE HOME" COMMAND
77 A=A-1
78 GOTO 45
80 A$=CHR$(INP(N))                  ' READ DATA FROM THE DMC-400
85 IF A$<>CHR$(10) THEN PRINT A$:
90 IF A$=CHR$(63) THEN 18
94 GOTO 45
95 NEXT I
100 PRINT "LEAVE THE X/Y CONTROLS ALONE AND CHECK TO INSURE THAT X & Y =0"
102 PRINT
105 INPUT "PRESS ( P ) WHEN READY":F$
110 IF F$="P" THEN 199
115 GOTO 105
129 PRINT
130 INPUT "HAS THE ORIGIN BEEN CORRECTLY DEFINED? (Y/N)":D$
135 IF D$="Y" THEN 145
140 GOTO 16
144 PRINT
145 PRINT "YOU ARE NOW READY TO BEGIN TAKING DATA.  MOVE THE VIEWER OVER"
146 PRINT "THE DESIRED POSITION AND PRESS ( DH ) TO CATALOG THE POINT.  START"
147 PRINT "WITH THE BASELINE, THEN SCALING POINTS, THEN THE SHORELINE POINTS."
148 PRINT
199 I=1
200 FOR I=1 TO 5 STEP 2            ' LOOP TO TAKE X/Y DATA
210 J=I-1
220 N=1000+J
222 PRINT
225 PRINT "PRESS ( DH ) TO CATALOG ":N:" ADDRESS DATA."
230 GOSUB 500                      ' SUBROUTINE TO COMMUNICATE W/DMC-400
250 IF N=1000 THEN 260
257 GOTO 270
```

```
260 X=(-1)*R
265 GOTO 278
270 IF N=1202 THEN 272
271 GOTO 275
272 Y=R*(-1)
273 GOTO 278
275 Z=R
278 NEXT I
279 PRINT
280 PRINT "YOUR X,Y & Z COORD'S ARE ";X,Y,Z
281 INPUT "WOULD YOU LIKE TO STORE THESE PTS IN THE DATA FILE (Y/N):";Y$
282 IF Y$="N" THEN 289
283 PRINT #1,X;Y;Z
284 COUNT=COUNT+1
285 IF X=0 THEN 129
286 IF Y=0 THEN 129
289 PRINT
290 INPUT "WOULD YOU LIKE TO CATALOG MORE DATA POINTS? (Y/N)";G$
300 IF G$()"N" THEN 148
302 PRINT
303 PRINT "THERE ARE ";COUNT;" POINTS STORED IN FILE ";E$
304 PRINT
305 PRINT "BE SURE TO LOG THIS INFORMATION, AS YOU WILL NEED IT LATER !"
306 PRINT
308 PRINT "THAT'S ALL FOLKS!!! ITS MILLER TIME !!!"
309 CLOSE
310 END
500 REM THIS IS A SUBROUTINE TO COMMUNICATE BETWEEN THE DMC-400 $ IBM PC
502 A=1                                    ' THIS SUBROUTINE COMMANDS THE DMC-400
505 M=6                                    ' TO REPORT ITS POSITION (TELL POSITION
510 R=0                                    ' COMMAND), AND THEN READS THE POSITION
515 K=1                                    ' FROM THE N ADDRESS. THE POSITION (IN
520 PRINT CHR$(INP(N));
530 B=INP(N+1)
540 C=INT(B/2)
550 IF C=B/2 THEN 565                      ' CHECKING STATUS & READING DATA
555 IF INT(C/2)=C/2 THEN 530
556 IF A=4 THEN 690                        ' AXIS COUNTER 1=X   2=Y
557 A$=INKEY$
558 IF LEN(A$)=0 THEN 530                  ' ASSIGN "TELL POSITION COMMAND"
559 PRINT A$;
560 OUT N, ASC(A$)                         ' SEND COMMAND TO DMC-400
562 A=A+1
564 GOTO 530
565 A$=CHR$(INP(N))
566 IF A$()CHR$(10) THEN PRINT A$;
568 IF A$=CHR$(63) THEN 502
570 V=ASC(A$)
580 IF (V)=48) AND (V(=57) THEN 620        ' CHECKING TO SEE IF DATA ARE
590 IF (V)=65) AND (V(=70) THEN 620        ' CHARACTERS 0-9 OR A-F
610 GOTO 530
620 IF V(60 THEN Z=(V-48)                  ' CHANGING FROM HEX TO DEC
630 IF V)60 THEN Z=(V-55)
640 R=R+(Z*16^(M-1))
645 IF M=6 THEN Z2=Z
650 M=M-1
660 IF K=6 THEN 690
672 K=K+1
680 GOTO 530
690 IF Z2 < 8 THEN 710
700 R=R-16777216#
710 RETURN
```

APPENDIX B
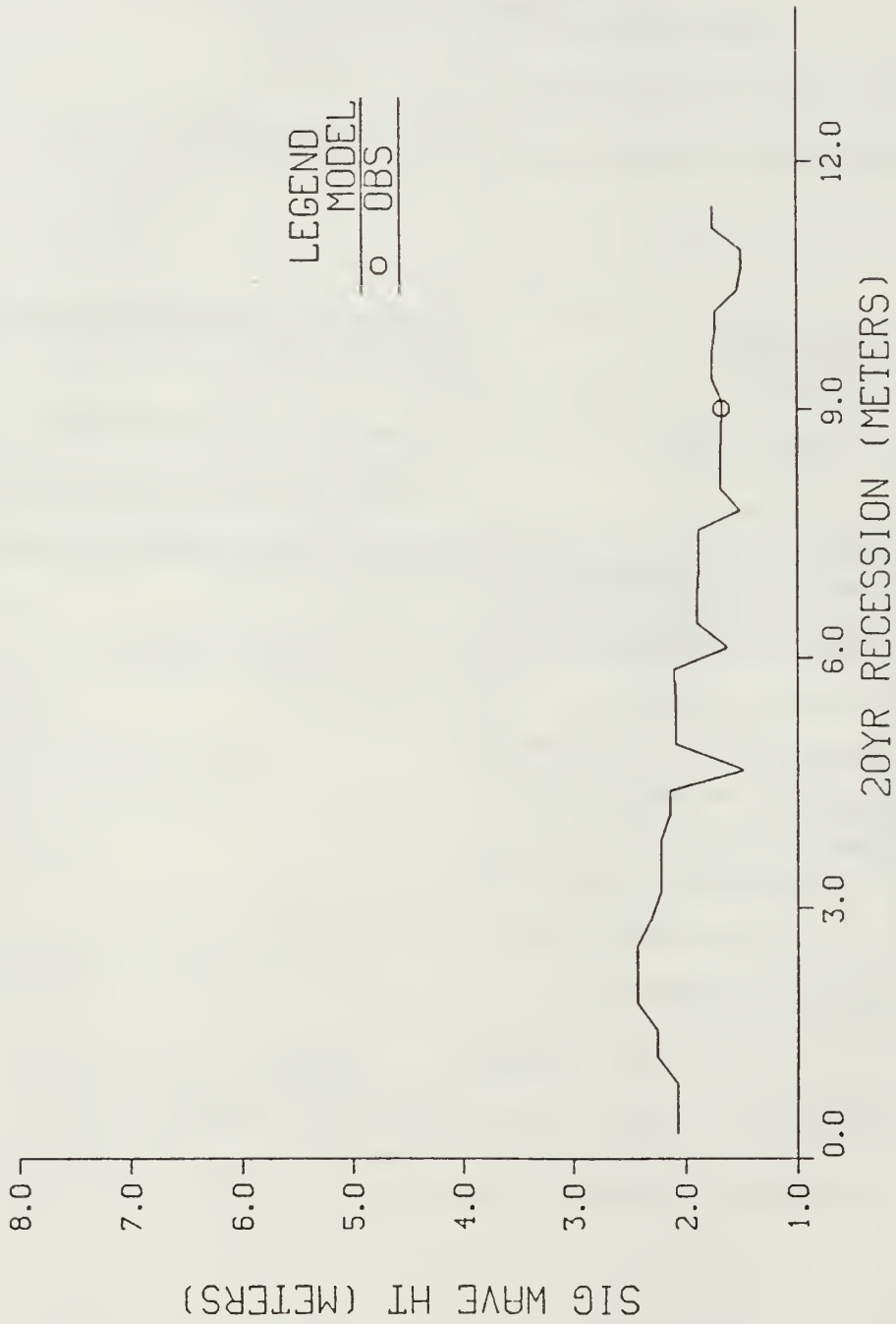
PROGRAM LISTING WRKPROG

```
10 INPUT "INPUT THE NUMBER OF POINTS IN THE DATA FILE:";N
20 DIM X#(N),Y#(N),Z#(N),XR#(N),YR#(N)
30 PRINT
40 INPUT "INPUT THE NAME OF YOUR DATA FILE, I.E. LAB1933:";E$
45 PRINT
50 OPEN "I",#1,E$
70 FOR I=1 TO N
80 INPUT #1,X#(I),Y#(I),Z#(I)
90 NEXT I
98 I=1
100 AX#=.000123763875#              ' REGRESSION COEFFICIENTS TO CONVERT
105 BX#=-.00072479248#              ' ENCODER COUNTS TO CENTIMETERS, WHERE
110 AY#=.000092559173#              ' CM = A*(E-COUNTS) + B
115 BY#=-.00513239147#
150 FOR I=2 TO N
160 X#(I)=X#(I)*AX# + BX#                 ' CONVERSION E-COUNTS TO CM
170 Y#(I)=Y#(I)*AY# + BY#
190 NEXT I
200 ALFA#=ATN(Y#(2)/X#(2))                ' COORDINATE SYS ROTATION ANGLE
210 FOR J=1 TO N
220 XR#(J)=(X#(J)*COS(ALFA#))+(Y#(J)*SIN(ALFA#))  ' COORDINATE TRANSFORMATION
230 YR#(J)=((-1)*X#(J)*SIN(ALFA#))+(Y#(J)*COS(ALFA#))
240 NEXT J
245 PRINT
248 INPUT "INPUT THE MEASURED FIELD DISTANCE (IN METERS):";GDIST
250 PRINT
270 PDIST#=SQR((XR#(4)-XR#(3))^2 + (YR#(4)-YR#(3))^2)
274 LPRINT
275 LPRINT "PHOTODISTANCE = ";PDIST#;" CM"
277 PRINT
280 PSCALE#=(PDIST#/100)/GDIST
283 PRINT PSCALE#
285 P#=1/PSCALE#
289 LPRINT
290 LPRINT "PHOTOSCALE IS: ";P#
291 LPRINT
292 LPRINT "YOUR ACTUAL SCALE, ROTATED X/Y PAIRS FOLLOW (METERS)"
300 FOR K= 5 TO N
310 XR#(K)= (XR#(K)/PSCALE#)/100
320 YR#(K)= (YR#(K)/PSCALE#)/100
335 LPRINT XR#(K),YR#(K)
350 NEXT K
360 LPRINT
400 FOR L = 5 TO (N-1)                    ' TRAPAZOIDAL RULE INTEGRATION
420 AREA#=AREA# + ((YR#(L)+YR#(L+1))/2)*ABS(XR#(L+1)-XR#(L))
450 NEXT L
460 PRINT
500 LPRINT "THE AREA IS: ";AREA#;" SQUARE METERS FOR STATION ";E$
600 CLOSE
900 END
```
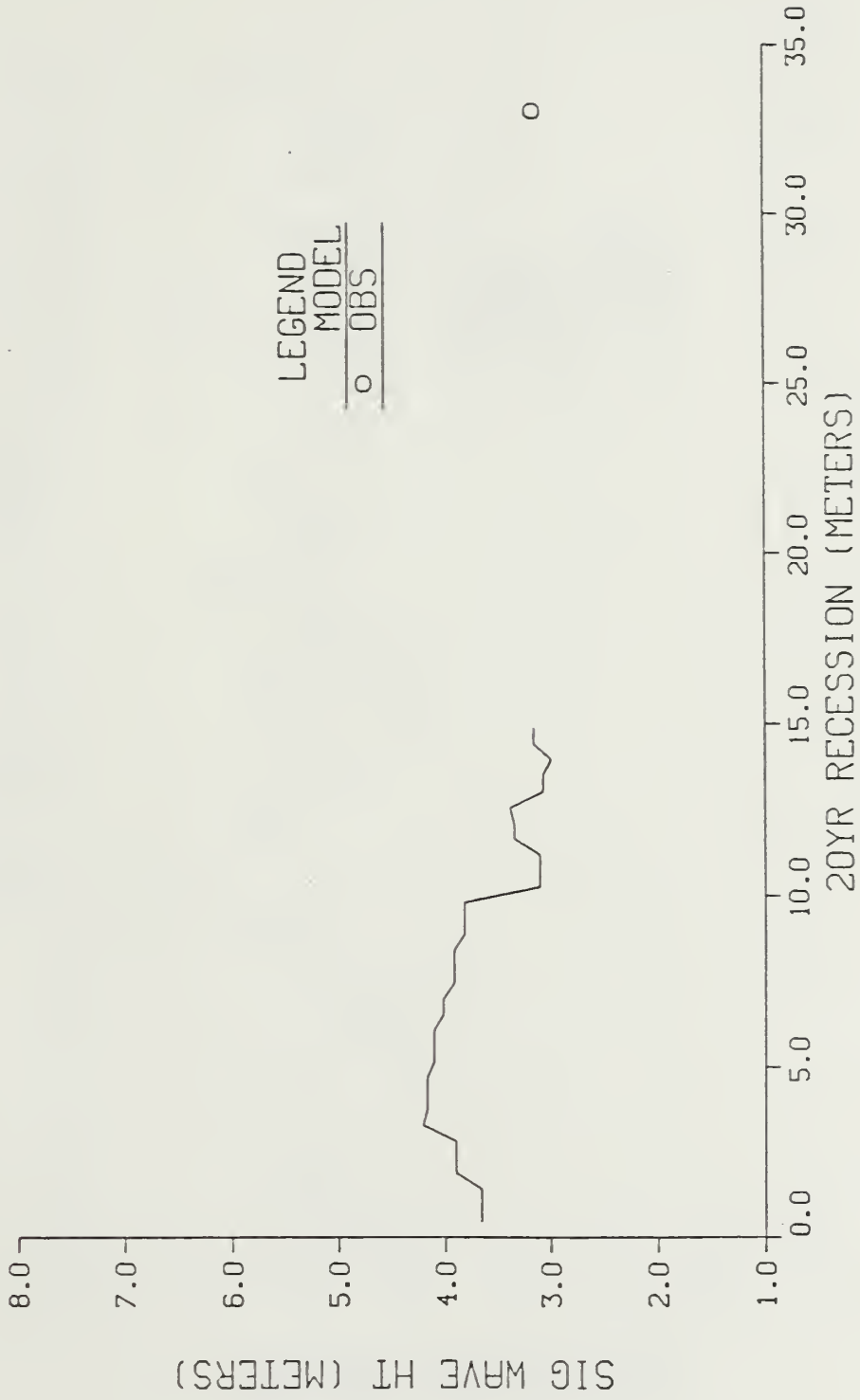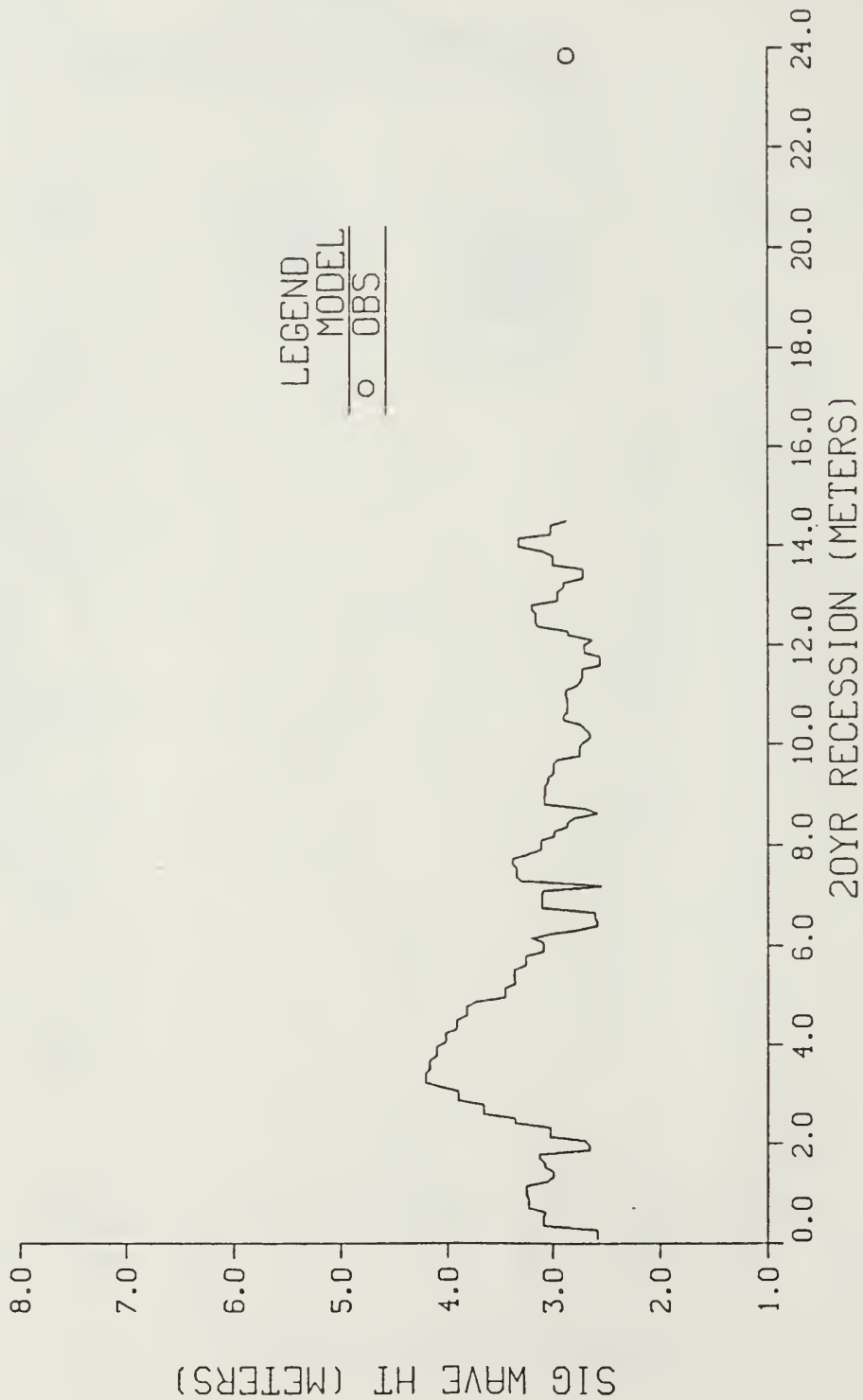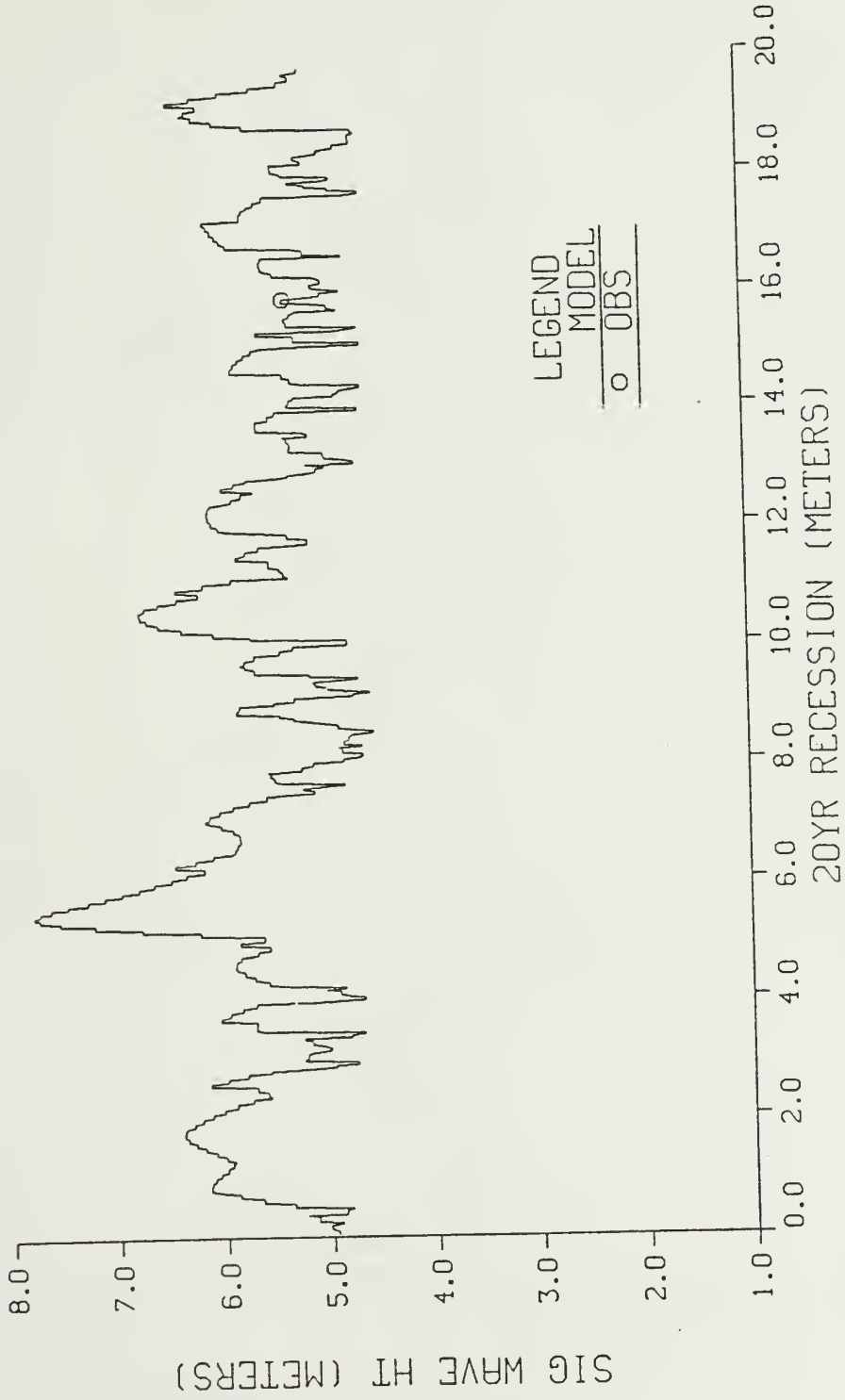
BEACH LAB

MONTEREY SAND COMPANY

SIG WAVE HT (METERS)

20YR RECESSION (METERS)

LEGEND
MODEL
o OBS

77

SAND CITY

LEGEND
MODEL
○ OBS

20YR RECESSION (METERS)

SIG WAVE HT (METERS)

SOUTH FORT ORD

SIG WAVE HT (METERS)

20YR RECESSION (METERS)

LEGEND
MODEL
o OBS

79

STILLWELL HALL

LEGEND
MODEL
o   OBS

SIG WAVE HT (METERS)

20YR RECESSION (METERS)

80

MARINA

SIG WAVE HT (METERS)

20YR RECESSION (METERS)
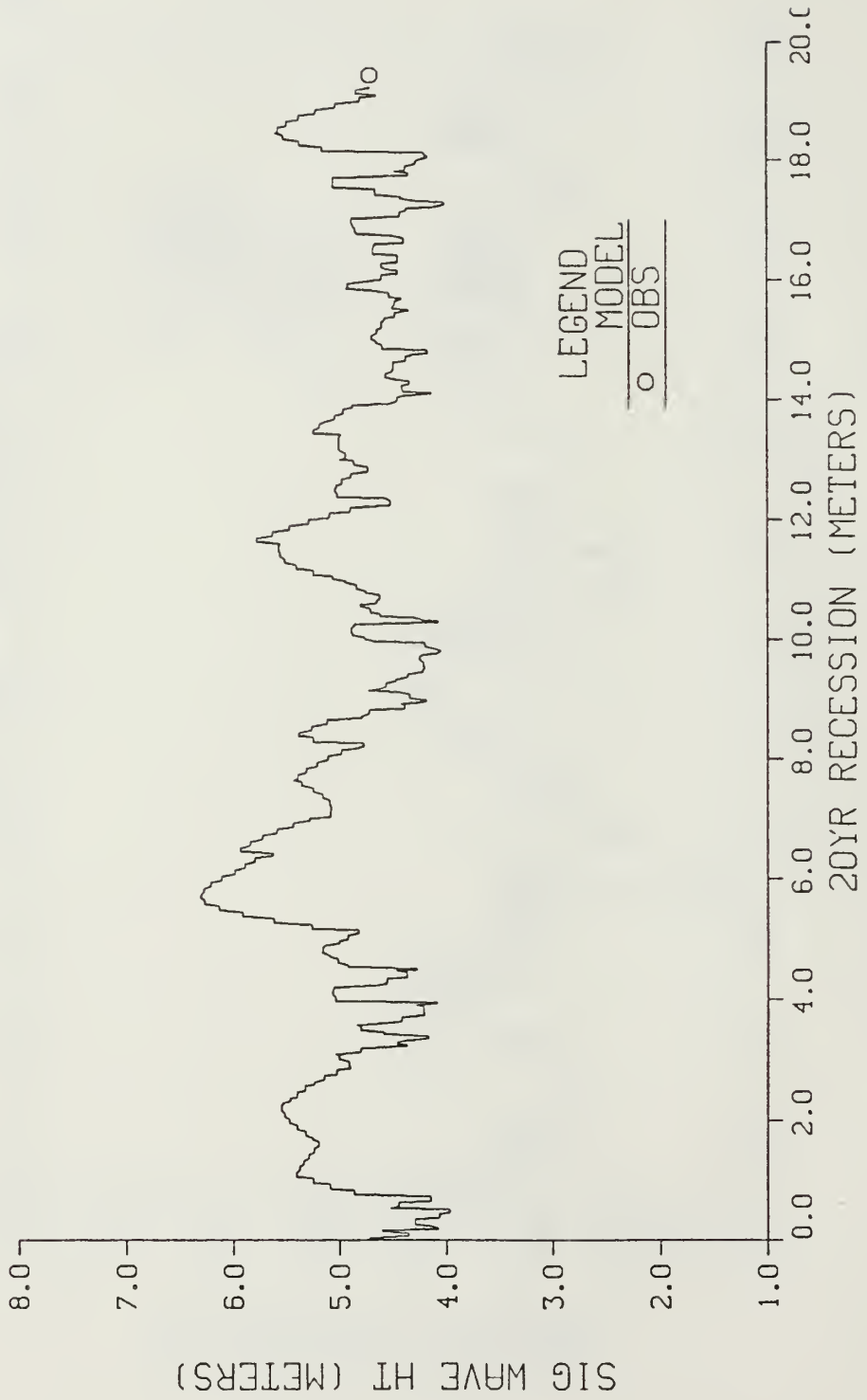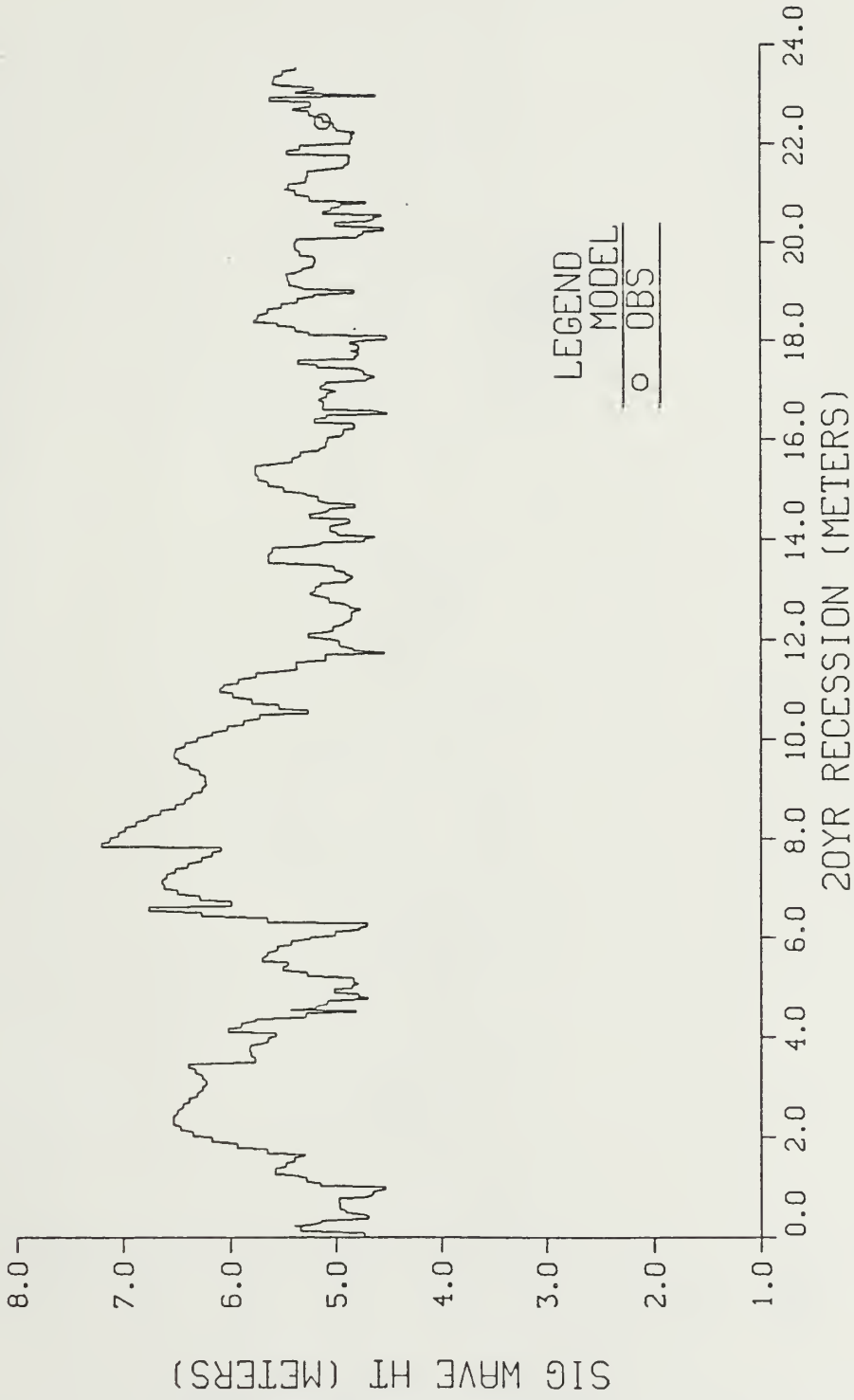
LEGEND
MODEL
○ OBS

RINCON BEACH

LEGEND
MODEL
o OBS

SIG WAVE HT (METERS)

20YR RECESSION (METERS)

82

ZMUDOWSKI DUNES

SIG WAVE HT (METERS)

20YR RECESSION (METERS)

LEGEND
MODEL
○ OBS
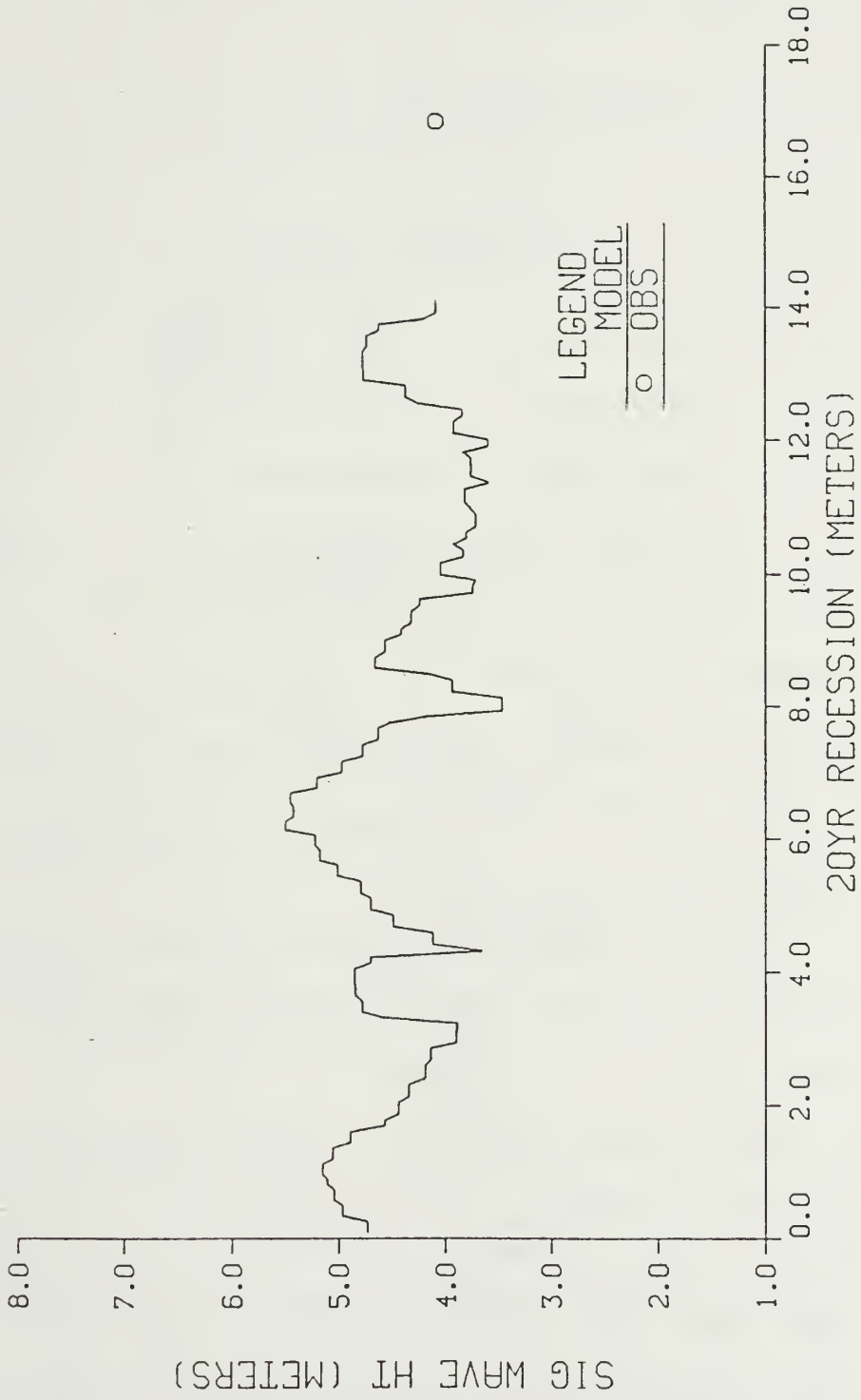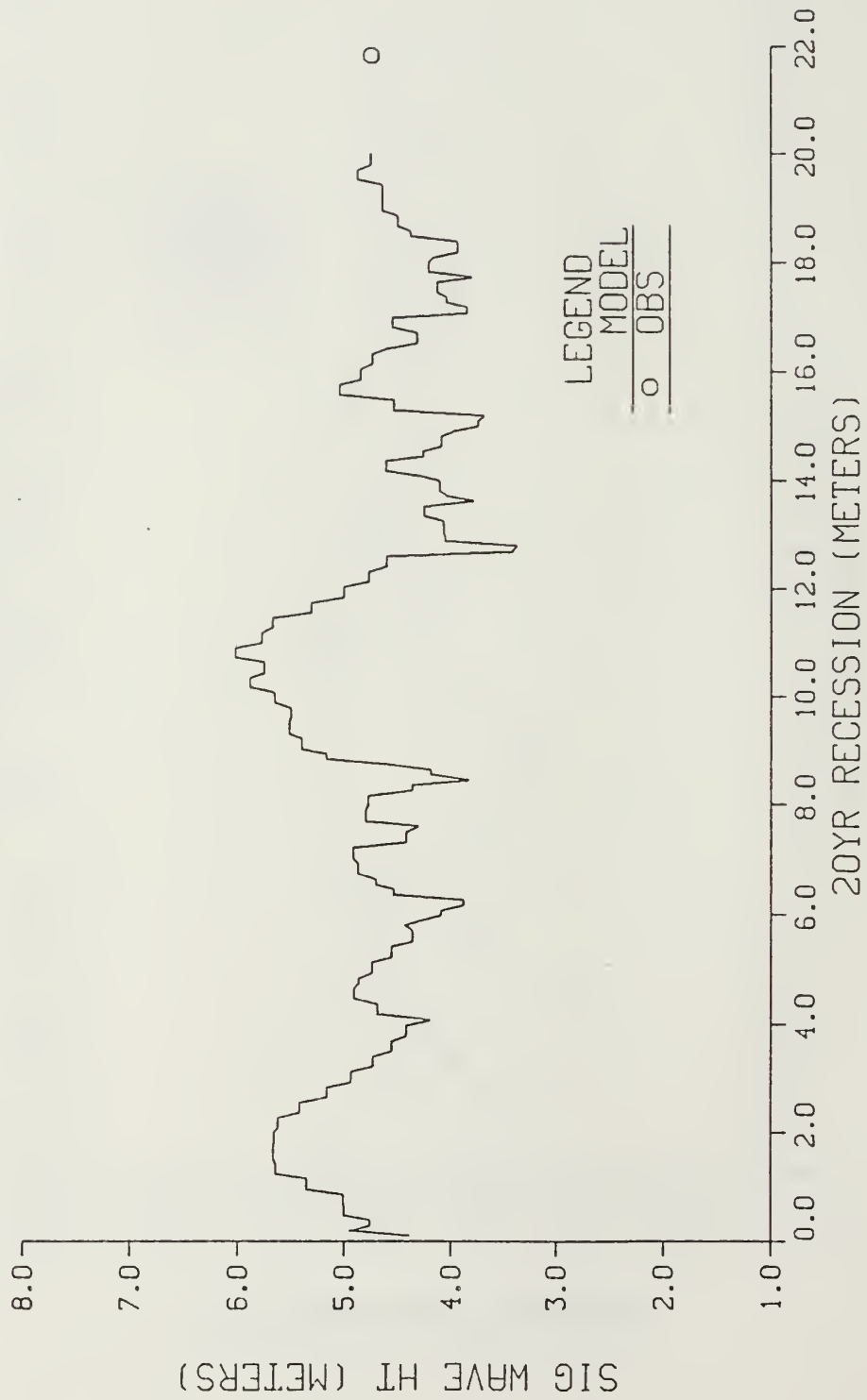
83

MONTEREY BAY ACADEMY

84
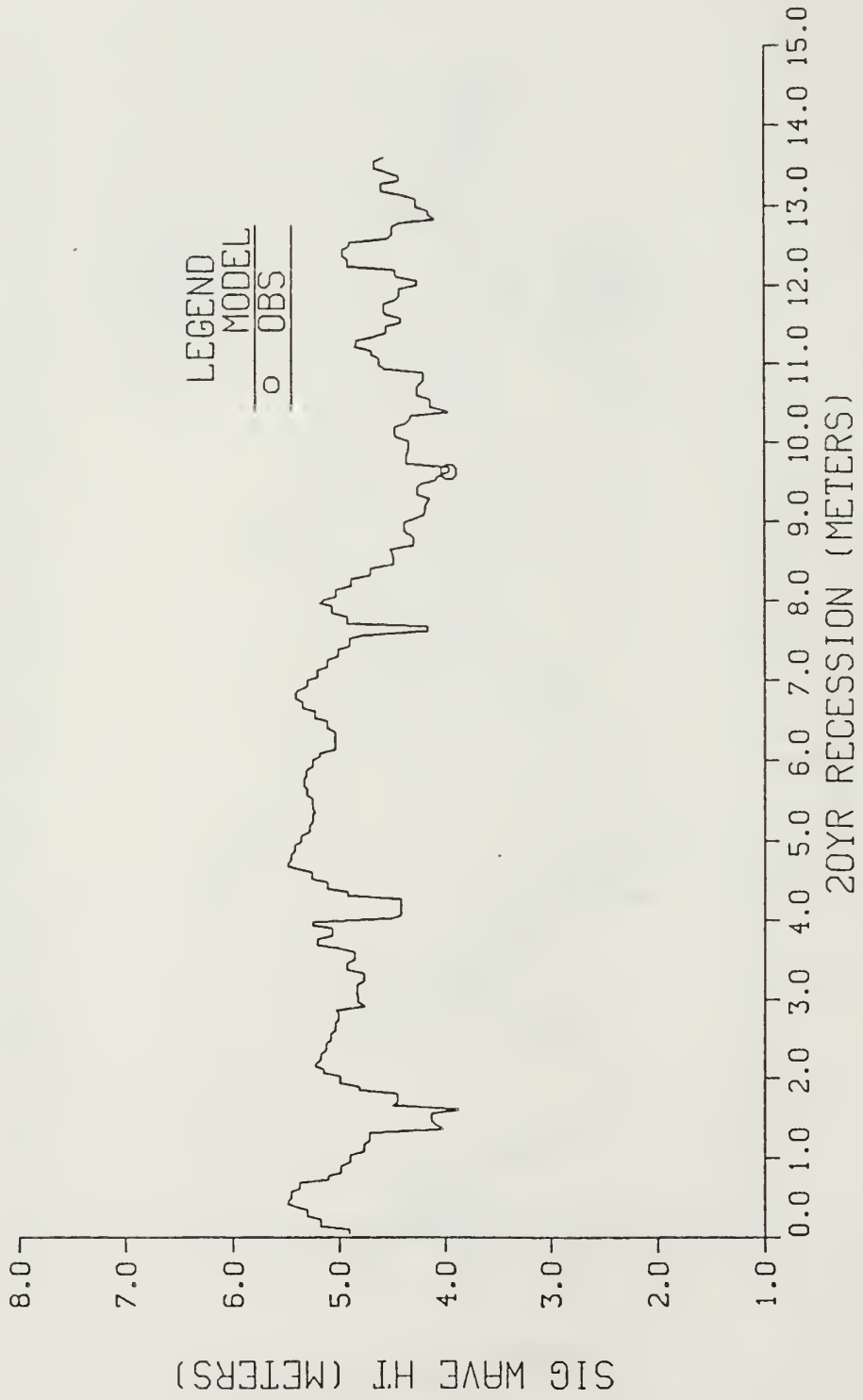
LIST OF REFERENCES

Barnet, T.P., On the Generation, Dissipation, and Prediction of Wind Waves, *Journal Geophysical Research*, 73, 1968.

Dennis, R.E., and E.E. Long, A Users Guide to a Computer Program for Harmonic Analysis of Data at Tidal Frequencies, *NOAA Technical Report*, *NOS 41*, 1971.

Dexter, P.E., Tests of Some Programmed Numerical Wave Forecast Models, *Journal Physical Oceanography*, 4, 1974.

Dobson, R.S., Some Applications of a Digital Computer to Hydraulic Engineering Problems, *Technical Report 80*, Stanford University, 1967.

Franke, R., personal communication with Ms. D. Burych regarding triangulation scheme smoothing, March 1986.

Griggs, G., and L. Savoy, *Living with the California Coast*, Duke University Press, 1985

Guza, R.T., and E.B. Thornton, Wave Set-up on a Natural Beach, *Journal Geophysical Research*, 86 (C5), 1981.

Hallert, B., *Photogrammetry*, *Basic Principles and General Survey*, McGraw-Hill Book Company Inc., 1960.

Hasselmann, K., On the Non-linear Energy Transfer in a Gravity-wave Spectrum-general Theory, *Journal Fluid Mechanics*, 12, Part 1, 1962.

Heinzen, M.R., *Hydrographic Surveys*: *Geodetic Control Criteria*, Thesis, Cornell University, 1977

Holman, R.A., and A.H. Sallenger, Set-up and Swash on a Natural Beach, *J. Geophysical Research*, 90 (C1), 1985.

Jones, G.B., *Coastal Erosion at Selected Points on Southern Monterey Bay*, Senior Thesis, University of California, Santa Cruz, 1983.

Keuffel and Esser, *Operating Manual for the Ranger-IV Electronic Distance Measuring Instrument*, Keuffel and Esser Co., 1975.

Komar, D.P., *Handbook of Coastal Processes and Erosion*, CRC Press, 1983.

Komar, D.P., and R.A. Homan, Coastal Processes and the Development of Shoreline Erosion, *Annual Review Earth Planetary Sciences*, 14, 1986.

Lima Blanco, W.R., and H.I. Sklavidis, *Coastal Erosion Along Monterey Bay*, Master's Thesis, Naval Postgraduate School, March 1985.

Miles, J.W., On the Generation of Surface Waves by Shear Flows, *J. Fluid Mechanics*, 3, 1957.

Moffitt, F.H., History of Shoreline Growth and Analysis of Aerial Photographs, *Technical Report HEL-2-21*, 1968.

Moffitt, F.H., and E.M. Mikhail, *Photogrammetry*, 3rd edition, Harper and Row, 1980.

Oradiwe, E., *A Sand Budget for Monterey Bay*, Master's Thesis, Naval Postgraduate School, March 1986

Phillips, O.M., On Generation of Waves by Turbulents Wind, *Journal Fluid Mechanics*, 2, 1957.

Reisio, D.T., and C.L. Vincent, A Comparison of Various Numerical Wave Perdiction Techniques *Marine Technical Society and American Society of Civil Engineers Paper 3642*, 1979.

Reisio, D.T., On Estimation of Wind-wave Generation in a Discrete Spectral Model, *Journal Physical Oceanography*, 4, 1981.

Reisio, D.T., C.L. Vincent, and W.D. Corson, Objective Specification of Atlantic Ocean Wind Fields from Historical Data, *WIS Report 4*, U.S. Army Engineer Waterways Experiment Station, 1982.

Schureman, P., *Manual of Harmonic Analysis and Prediction of Tide*, U.S. Government Printing Office, 1971.

Thompson, W.C., Report on Coast Erosion and Run-up on Phillips Petroleum Property, prepared for Ponderosa Homes, Santa Clara, 1981.

Thornton, E.B., Preliminary Report on Waves at Halfmoon Bay, prepared for Severson, Werson, Berke, and Melchior, 1983.

Thornton, E.B., M. Asce, A.J. Sklavidis, W. Lima Blanco, D.M. Burych, S.P. Tucker, and D. Puccini, Coastal Erosion along Monterey Bay, *Technical Report*, U.S. Army Corps of Engineers, 1985.

INITIAL DISTRIBUTION LIST

		No. Copies
1.	Defense Technical Information Center Cameron Station Alexandria, VA 22304-6145	2
2.	Library, Code 0142 Naval Postgraduate School Monterey, CA 93943-5002	2
3.	Chairman, Department of Oceanography Code 68 Naval Postgraduate School Monterey, CA 93943-5000	1
4.	Chairman, Department of Meteorology Code 63 Naval Postgraduate School Monterey, CA 93943-5000	1
5.	NOAA Liaison Officer Post Office Box 8688 Monterey, CA 93943-0688	1
6.	Office of the Director Naval Oceanography Division (OP-952) Department of the Navy Washington, D.C. 20350	1
7.	Commander Naval Oceanography Command NSTL, MS 39522	1
8.	Commanding Officer Naval Oceanographic Office Bay St. Louis NSTL, MS 39522	1
9.	Commanding Officer Naval Ocean Research and Development Activity Bay St. Louis NSTL, MS 39522	1
10.	Chief of Naval Research 800 N. Quincy Street Arlington, VA 22217	1
11.	Chairman, Oceanography Department U.S. Naval Academy Annapolis, MD 21402	1
12.	Director, Defense Mapping Agency Hydrographic/Topographic Center 6500 Brookes Lane Washington, D.C. 20315	1
13.	Chief, Nautical Charting Division N/CG2, Room 1026, WSC-1 National Oceanic and Atmospheric Administration Rockville, MD 20852	1

14.	Chief, Hydrographic Surveys Branch N/CG24, Room 404, WSC-1 National Oceanic and Atmospheric Administration Rockville, MD 20852	1
15.	Director, Pacific Marine Center N/MOP National Ocean Service, NOAA 1801 Fairview Avenue, East Seattle, WA 98102	1
16.	Director, Atlantic Marine Center N/MOA National Ocean Service, NOAA 439 West York Street Norfolk, VA 23510	1
17.	Dr. Edward B. Thornton Code 68 Naval Postgraduate School Monterey, CA 93943-5100	3
18.	Dr. Stevens Tucker Code 68Tx Naval Postgraduate School Monterey, CA 93943-5100	3
19.	Mr. Thomas Kendall Corps of Engineers SPNPE-W 211 Main St. San Francisco, CA 94111	1
20.	Prof. Gary Griggs Department Chairman Department of Air Sciences University of California Santa Cruz, CA 95064	1
21.	Mr. Stan Stevens Map and Photo Library University of California Santa Cruz, CA 95064	1
22.	Dr. Douglas L. Inman Scripps Institution of Oceanography Geological Research Division University of California La Jolla, CA 92073	1
23.	Mr. Reed S. Armstrong National Marine Fisheries Services Atlantic Environmental Group Narraganset, RI 02882	1
24.	Mr. Warren Thompson 830 Dry Creek Road Monterey, Ca 93940	1
25.	Dr. R.L. Weigel Department of Civil Engineering University of California Berkley, CA 94720	1
26.	Dr. R. Flick Scripps Institution of Oceanography Code A009 University of California La Jolla, CA 92073	1

27.   LCDR Tim McGee   1
       NAVOCEANCOMDET
       Diego Garcia
       FPO San Francisco 96685-2000